Molecular Biology of the Cell
Vol. 14, 4051–4066, October 2003

The Role of Cdc42p GTPase-activating Proteins in Assembly of the Septin Ring in Yeast

Juliane P. Caviston,* Mark Longtine,† John R. Pringle,‡ and Erfei Bi*§

*Department of Cell and Developmental Biology, University of Pennsylvania School of Medicine, Philadelphia, Pennsylvania 19104-6058; †Department of Biochemistry and Molecular Biology, Oklahoma State University, Stillwater, Oklahoma 74078-3035; and ‡Department of Biology, University of North Carolina, Chapel Hill, North Carolina 27599-3280

Submitted April 21, 2003; Revised June 13, 2003; Accepted June 13, 2003
Monitoring Editor: Tim Stearns

The septins are a conserved family of GTP-binding, filament-forming proteins. In the yeast *Saccharomyces cerevisiae*, the septins form a ring at the mother-bud neck that appears to function primarily by serving as a scaffold for the recruitment of other proteins to the neck, where they participate in cytokinesis and a variety of other processes. Formation of the septin ring depends on the Rho-type GTPase Cdc42p but appears to be independent of the actin cytoskeleton. In this study, we investigated further the mechanisms of septin-ring formation. Fluorescence-recovery-after-photobleaching (FRAP) experiments indicated that the initial septin structure at the presumptive bud site is labile (exchanges subunits freely) but that it is converted into a stable ring as the bud emerges. Mutants carrying the *cdc42*^{V36G} allele or lacking two or all three of the known Cdc42p GTPase-activating proteins (GAPs: Bem3p, Rga1p, and Rga2p) could recruit the septins to the cell cortex but were blocked or delayed in forming a normal septin ring and had accompanying morphogenetic defects. These phenotypes were dramatically enhanced in mutants that were also defective in Cla4p or Gin4p, two protein kinases previously shown to be important for normal septin-ring formation. The Cdc42p GAPs colocalized with the septins both early and late in the cell cycle, and overexpression of the GAPs could suppress the septin-organization and morphogenetic defects of temperature-sensitive septin mutants. Taken together, the data suggest that formation of the mature septin ring is a process that consists of at least two distinguishable steps, recruitment of the septin proteins to the presumptive bud site and their assembly into the stable septin ring. Both steps appear to depend on Cdc42p, whereas the Cdc42p GAPs and the other proteins known to promote normal septin-ring formation appear to function in a partially redundant manner in the assembly step. In addition, because the eventual formation of a normal septin ring in a *cdc42*^{V36G} or GAP mutant was invariably accompanied by a switch from an abnormally elongated to a more normal bud morphology distal to the ring, it appears that the septin ring plays a direct role in determining the pattern of bud growth.

INTRODUCTION

The septin family of proteins was first recognized in yeast and now appears to be ubiquitous in fungi and animals, although not in plants (Longtine *et al.,* 1996; Field and Kellogg, 1999; Trimble, 1999; Nguyen *et al.,* 2000; Momany *et al.,* 2001; Macara *et al.,* 2002). Typical septins have a variable N-terminal region, a conserved core that includes the elements of a GTP-binding site, and a variable C-terminal region that (in all but a few cases) includes a predicted coiled-coil domain. In each species examined to date, there are two or more septins that form heterooligomeric complexes to perform their specific functions. Purified septins from yeast, *Drosophila*, *Xenopus*, and mammalian cells form filaments of 7–9 nm diameter and of variable length (Field *et al.,* 1996; Frazier *et al.,* 1998; Hsu *et al.,* 1998; Kinoshita *et al.,* 2002; Mendoza *et al.,* 2002).

In *Saccharomyces cerevisiae*, there are seven septin genes, of which five (*CDC3, CDC10, CDC11, CDC12,* and *SHS1/SEP7*) are expressed in vegetative cells (Longtine *et al.,* 1996; Carroll *et al.,* 1998; Mino *et al.,* 1998) and two (*SPR3* and *SPR28*) only during sporulation (DeVirgilio *et al.,* 1996; Fares *et al.,* 1996). The five vegetatively expressed septins have identical localization patterns throughout the cell cycle. They are recruited to the presumptive bud site and form a ring there; as the bud emerges, the ring becomes an hourglass structure that spans the mother-bud neck until the time of cytokinesis, when it splits into two distinct rings that transiently mark the division sites on both mother and daughter cells (Ford and Pringle, 1991; Kim *et al.,* 1991; Lippincott *et al.,* 2001). (For convenience, in most of this article, we use "ring" to refer to both the prebudding ring and the hourglass structure; the stages in formation of the mature structure are considered further in the DISCUSSION) Localization of the septins to the neck is interdependent, with inactivation of one septin generally preventing the other septins from localizing normally (Haarer and Pringle, 1987; Ford and Pringle, 1991; Kim *et al.,* 1991; Longtine *et al.,* 1996). Electron microscopy has shown that the neck contains a seemingly filamentous structure whose localization coincides with that of the septins from bud emergence until cytokinesis (Byers and Goetsch, 1976a; Byers, 1981). These "neck filaments" are lost in temperature-sensitive (Ts^-) septin mutants at the nonpermissive temperature (Byers and Goetsch, 1976b;

Article published online ahead of print. Mol. Biol. Cell 10.1091/mbc.E03–04–0247. Article and publication date are available at www.molbiolcell.org/cgi/doi/10.1091/mbc.E03–04–0247.

§ Corresponding author. E-mail address: ebi@mail.med.upenn.edu.

Byers, 1981). Taken together, the evidence suggests that the septins are the major constituents of the neck filaments.

One major role for the septins in various organisms is in cytokinesis (Hartwell, 1971; Neufeld and Rubin, 1994; Kinoshita *et al.*, 1997; Bi *et al.*, 1998; Lippincott and Li, 1998). Consistent with this, the septins typically localize to the division site (cleavage furrow) at least during the cytokinesis phase of the cell cycle (Longtine *et al.*, 1996; Field and Kellogg, 1999; Trimble, 1999; Nguyen *et al.*, 2000; Westfall and Momany, 2002). However, the precise molecular role(s) of the septins in cytokinesis have not yet been elucidated in any cell type.

The septins also appear to have other functions in both yeast and animal cells. For example, considerable evidence suggests that the septins are involved in one or more steps of vesicle trafficking in mammalian cells (Hsu *et al.*, 1998; Beites *et al.*, 1999; Kartmann and Roth, 2001; Dent *et al.*, 2002). In yeast, the septins play roles in bud-site selection, the spatial organization of cell-wall deposition, and the "morphogenesis checkpoint" that couples cell-cycle progression to progress in bud formation (Chant *et al.*, 1995; Sanders and Herskowitz, 1996; DeMarini *et al.*, 1997; Barral *et al.*, 1999; Shulewitz *et al.*, 1999; Longtine *et al.*, 2000; Schenkman *et al.*, 2002). Proteins involved both in cytokinesis and in these other diverse processes are targeted to the mother-bud neck in a septin-dependent manner with a variety of temporal and spatial patterns (Gladfelter *et al.*, 2001b). Thus, the septins have been proposed to function as a scaffold at the neck for protein anchoring and organization (Longtine *et al.*, 1996, 1998a; Field and Kellogg, 1999; Gladfelter *et al.*, 2001b). In addition, the septins appear to provide a diffusion barrier at the neck that prevents membrane-associated proteins from moving freely between the mother and bud compartments (Barral *et al.*, 2000; Takizawa *et al.*, 2000). Because all functions of the septins in vegetative yeast cells appear to involve their localization and proper organization at the mother-bud neck, it is crucial to elucidate the mechanisms by which the normal septin ring is formed.

Several proteins are known to affect septin-ring formation in yeast. The Rho-family GTPase Cdc42p and its activating factor (GEF) Cdc24p are required for the polarized assembly of both the actin cytoskeleton and the septins at the beginning of the cell cycle (Pringle *et al.*, 1995; Johnson, 1999; Pruyne and Bretscher, 2000; Cid *et al.*, 2001; Gladfelter *et al.*, 2001a). However, actin and the septins appear to be independent of each other for their organization at the presumptive bud site (Adams and Pringle, 1984; Ford and Pringle, 1991; Ayscough *et al.*, 1997; Harkins *et al.*, 2001). In the past decade, a major effort has focused on how Cdc42p controls actin organization (Johnson, 1999; Pruyne and Bretscher, 2000), but studies of the role of Cdc42p in septin organization have lagged behind. Detailed analyses of panels of site-directed *cdc42* mutants have revealed a class of mutations that causes defects in septin organization and a cell morphology resembling that of septin mutants (Kozminski *et al.*, 2000; Gladfelter *et al.*, 2001a). Further study of two *cdc42* effector-loop mutants and of the roles of Bem3p, Rga1p, and Rga2p, which are three GTPase-activating proteins (GAPs) for Cdc42p (Zheng *et al.*, 1993; Stevenson *et al.*, 1995; Johnson, 1999; Smith *et al.*, 2002), has suggested that Cdc42p GTPase cycling is involved in septin-ring formation (Gladfelter *et al.*, 2002). In particular, it was suggested that Cdc42p, like the assembly GTPase EF-Tu in protein synthesis, participates in septin-ring formation by shuttling septin complexes to the assembling ring structure (Gladfelter *et al.*, 2002), a view that contrasts with the more common view of activated (i.e., GTP-bound) Cdc42p activating effectors in signaling pathways in a Ras-like manner (Johnson, 1999).

In addition to Cdc42p, its GEF, and its GAPs, several other proteins including Bni5p, Nap1p, and the protein kinases Cla4p, Gin4p, and Elm1p are also known to be involved in formation of the normal septin ring (Cvrcková *et al.*, 1995; Longtine *et al.*, 1998a, 2000; Sreenivasan and Kellogg, 1999; Bouquin *et al.*, 2000; Weiss *et al.*, 2000; Lee *et al.*, 2002). Cla4p may function in the same pathway as Cdc42p, because it is a Cdc42p effector (Cvrcková *et al.*, 1995; Weiss *et al.*, 2000), although it is not clear whether the interaction between Cla4p and Cdc42p is required for its role in septin organization. It is even less clear how the other proteins affect septin organization.

In this study, we have focused on the role of the Cdc42p GAPs in septin-ring formation. We conclude that ring formation involves distinct steps of recruitment and assembly and that the Cdc42p GAPs are involved in the latter step.

MATERIALS AND METHODS

Strains, Growth Conditions, and Genetic Methods

Yeast strains used in this study are listed in Table 1; the construction of strains containing deletions and/or tagged genes is described below or in the table. Cells were grown on YM-P or YPD-rich liquid medium, solid YPD medium, or selective media (Lillie and Pringle, 1980; Guthrie and Fink, 1991), as indicated; 2% glucose was used as carbon source. G418/Geneticin (Life Technologies, Gaithersburg, MD) was used to select transformants containing the *kanMX6* marker (Longtine *et al.*, 1998b). *Escherichia coli* strain DH12S (Life Technologies) was used routinely as a plasmid host.

Standard methods of yeast genetics and recombinant-DNA manipulation (Sambrook *et al.*, 1989; Guthrie and Fink, 1991) were used except where noted. Restriction and DNA-modifying enzymes were purchased from New England BioLabs (Beverly, MA). *Taq*DNA polymerase and Expand High-Fidelity and Long-Template PCR Kits were purchased from Roche Diagnostics (Indianapolis, IN), and oligonucleotide primers were purchased from Integrated DNA Technologies (Coralville, IA). DNA sequencing was performed by the Sequencing Facility of the University of Pennsylvania.

Plasmid and Strain Constructions

Plasmids used in this study are listed in Table 2 or described where appropriate below. Plasmid YEp181-RGA1 was constructed by subcloning an ~5.8-kb *Hin*dIII fragment carrying *RGA1* from YEp24-RGA1 into the *Hin*dIII site of YEplac181. Plasmids pDLB1537 and pDLB1580, which carry the wild-type *RGA1* and $rga1^{K872A}$ alleles, respectively, in plasmid YEplac195 (Gietz and Sugino, 1988), were described by Gladfelter *et al.* (2002). Like YEp13-RGA1 and YEp24-RGA1 (see Figure 1), YEp181-RGA1 suppressed the *cdc12-6* allele, but pDLB1537 did not (unpublished data), probably because this plasmid contains less sequence upstream of *RGA1* (~340 base pairs) than do the other plasmids (~2.5 kb). Thus, the $rga1^{K872A}$ mutation was transferred into YEp181-RGA1 before suppression analyses. Plasmids pDLB1537 and pDLB1580 were digested with *Sac*I and *Nco*I, respectively, to linearize the plasmid DNAs without affecting the *RGA1* region. YEp181-RGA1 was digested with *Age*I and *Bgl*II, thus removing an internal 1539-base pair fragment that starts 1047 base pairs downstream of the *RGA1* start codon and then cotransformed into yeast strain YEF473A with the digested pDLB1537 or pDLB1580. "Gap-repaired" plasmids were identified by selecting Leu^+ Ura^- transformants, rescued into *E. coli* and confirmed by DNA sequencing, yielding plasmids YEp181-RGA1(WT) and YEp181-RGA1(K872A).

To construct plasmids carrying *CDC3-GFP*, *3HA-BEM3*, *GFP-BEM3*, *3HA-RGA1*, or *GFP-RGA1*, the wild-type genes were cloned into plasmid pALTER-1 (Promega, Madison, WI). Using the protocol recommended by Promega and the primers listed in Table 3, an in-frame *Not*I site was introduced immediately after the start codon of each gene except *CDC3*, in which the *Not*I site was inserted after codon 13. Finally, a *Not*I fragment carrying either GFP^{S65T} (DeVirgilio *et al.*, 1996) or *3HA* (Tyers *et al.*, 1993) was inserted at the introduced *Not*I site in each gene. Specifically, for *CDC3*, an ~4.5-kb *Eco*RI-*Sal*I fragment was subcloned from plasmid YEp102(CDC3)2 (Kim *et al.*, 1991) into *Eco*RI/*Sal*I-digested pALTER-1. After introducing *GFP* as just described, the ~5.3-kb *Eco*RI-*Sal*I fragment was subcloned into *Eco*RI/*Sal*I-digested YIplac211 (Gietz and Sugino, 1988), creating YIp211-CDC3-GFP, and into *Eco*RI/*Sal*I-digested pRS316, creating pRS316-CDC3-GFP. For *BEM3*, an ~4.3-kb *Xba*I fragment was subcloned from pPB547 (Table 2) into *Xba*I-digested pALTER-1. After introducing *3HA*, the ~4.4-kb *Xba*I fragment was

Table 1. Yeast strains used in this study

Strain	Genotype	Source
M-17	**a** *leu2 ura3 cdc12-6*	This study[a]
M-267	**a** *his3 leu2 lys2 trp1 ura3 gin4*Δ::*TRP1*	Longtine *et al.* (1998a)
M-1075	**a** *his3 leu2 lys2 trp1 ura3 swe1*::*LEU2*	This study[b]
YEF473	**a**/α *his3/his3 leu2/leu2 lys2/lys2 trp1/trp1 ura3/ura3*	Bi and Pringle (1996)
YEF473A	**a** *his3 leu2 lys2 trp1 ura3*	Bi and Pringle, 1996
YEF982	as YEF473 except *BEM3/bem3*Δ::*TRP1 RGA1/rga1*Δ::*HIS3*	This study[c]
YEF1026	α *his3 leu2 lys2 trp1 ura3 bem3*Δ::*TRP1 rga1*Δ::*HIS3*	Segregant from YEF982
YEF1035	**a** *his3 leu2 lys2 trp1 ura3 bem3*Δ::*TRP1 rga1*Δ::*HIS3*	Segregant from YEF982
YEF1209	**a** *his3 leu2 lys2 trp1 ura3 bem3*Δ::*HIS3 rgal*Δ::*HIS3*	This study[d]
YEF1300	α *his3 leu2 lys2 trp1 ura3 bem3*Δ::*HIS3 rga1*Δ::*HIS3 gin4*Δ::*TRP1*	Segregant from M-267 X YEF1209[e]
YEF1341	α *his3 leu2 lys2 trp1 ura3 ste20*Δ::*HIS3*	See text
YEF1343	α *his3 leu2 lys2 trp1 ura3 cla4*Δ::*HIS3*	See text
YEF1347	α *his3 leu2 lys2 trp1 ura3 skm1*Δ::*HIS3*	See text
YEF1381	**a** *his3 leu2 lys2 trp1 ura3 bem3*Δ::*TRP1 rga1*Δ::*HIS3 ste20*Δ::*HIS3*	Segregant from YEF1035 X YEF1341[f]
YEF1383	**a** *his3 leu2 lys2 trp1 ura3 bem3*Δ::*TRP1 rga1*Δ::*HIS3 cla4*Δ::*HIS3*	Segregant from YEF1035 X YEF1343
YEF1385	**a** *his3 leu2 lys2 trp1 ura3 bem3*Δ::*TRP1 rga1*Δ::*HIS3 skm1*Δ::*HIS3*	Segregant from YEF1035 X YEF1347
YEF1418	**a** *leu2 ura3 cdc12-6 ura3*::*3HA:RGA1-URA3*	This study[g]
YEF1423	as YEF473 except *bem3*Δ::*HIS3/bem3*Δ::*HIS3 ura3*::*3HA:BEM3-URA3/ ura3*::*3HA:BEM3-URA3*	This study[h]
YEF1424	as YEF473 except *rga1*Δ::*HIS3/rga1*Δ::*HIS3 ura3*::*3HA:RGA1-URA3/ ura3*::*3HA:RGA1-URA3*	This study[i]
YEF2288	as YEF473 except *RGA2/RGA2:GFP-KanMX6*	See text
YEF2291	as YEF473 except *RGA2:GFP-KanMX6/RGA2:GFP-KanMX6*	This study[j]
YEF2318	as YEF982 except *RGA2/rga2*Δ::*KanMX6*	See text
YEF2335	α *his3 leu2 lys2 trp1 ura3 bem3*Δ::*TRP1 rga1*Δ::*HIS3 rga2*Δ::*KanMX6*	Segregant from YEF2318
YEF2380	**a** *his3 leu2 lys2 trp1 ura3 bem3*Δ::*TRP1 rga1*Δ::*HIS3 rga2*Δ::*KanMX6*	Segregant from M-1075 X YEF2335
YEF2390	**a** *his3 leu2 lys2 trp1 ura3 bem3*Δ::*TRP1 rga1*Δ::*HIS3*	Segregant from YEF2318
YEF2517	α *his3 leu2 lys2 trp1 ura3 bem3*Δ::*HIS3 rga1*Δ::*HIS3 gin4*Δ::*TRP1*	Segregant from M-1075 X YEF1300
YEF2921	**a** *his3 leu2 lys2 trp1 ura3 cdc42*^{V36G}	This study[k]

[a] Derived by several crosses from the original *cdc12-6* strain (Adams and Pringle, 1984).

[b] Constructed as described for M-1077 (Longtine *et al.*, 2000).

[c] YEF1000 (Bi *et al.*, 2000) X YEF984 (like YEF992 [Bi *et al.*, 2000] except that *BEM3* was replaced by *TRP1* rather than *HIS3*).

[d] Segregant from YEF992 X YEF1000 (Bi *et al.*, 2000).

[e] Tetrads were dissected on a YPD plate containing 0.9 M KCl, which partially suppresses the *gin4*Δ defect (our unpublished results).

[f] YEF1035 harboring plasmid YEp352 was crossed to YEF1341 harboring plasmid YEp13, diploids were selected on an SC-Leu-Ura plate, and both plasmids were cured before tetrads were dissected.

[g] Plasmid YIp211-3HA-RGA1(see text) was linearized with *Apa*I and transformed into strain M-17, selecting for Ura$^+$, to integrate *3HA:RGAI* at the *ura3* locus.

[h] Plasmid YIp211-3HA-BEM3 (see text) was linearized with *Apa*I and transformed into strains YEF992 and YEF995 (Bi *et al.*, 2000), selecting for Ura$^+$, to integrate *3HA:BEM3* at the *ura3* locus. The *MAT***a** and *MATα* integrants were mated to form strain YEF1423.

[i] Plasmid YIp211-3HA-RGA1 (see text) was linearized with *Apa*I and transformed into strains YEF1000 and YEF1002 (Bi *et al.*, 2000), selecting for Ura$^+$, to integrate *3HA:RGA1* at the *ura3* locus. The *MAT***a** and *MATα* integrants were mated to form strain YEF1424.

[j] Constructed by mating two segregants from YEF2288.

[k] Constructed by replacing the *cdc42*Δ::*HIS3* allele in strain YEF1194 (Caviston *et al.*, 2002) with an ~1.7-kb *Bam*HI-*Sal*I fragment carrying *cdc42*^{V36G} from plasmid pRS314-CDC42-76 as described previously (Caviston *et al.*, 2002).

subcloned into *Xba*I-digested YIplac211 to create YIp211–3HA-BEM3. Similarly, after introducing *GFP*, the ~5.0-kb *Xba*I fragment was subcloned into pRS315, creating pRS315-GFP-BEM3 and used to replace the original ~4.3-kb *Xba*I fragment in pPB547, creating YEp13-GFP-BEM3. For *RGA1*, an ~5.8-kb *Hin*dIII fragment was subcloned from YEp13-RGA1 into *Hin*dIII-digested pALTER-1. After introducing *3HA*, an ~3.7-kb *Xho*I-*Hin*dIII fragment was subcloned into *Sal*I/*Hin*dIII-digested YIplac211 to create YIp211–3HA-RGA1. Similarly, after introducing *GFP*, the ~6.5-kb *Hin*dIII fragment was subcloned into *Hin*dIII-digested pRS315 to create plasmid pRS315-GFP-RGA1.

The tagged proteins appeared to be largely functional. Introduction of pRS316-CDC3-GFP into a *cdc3-3* temperature-sensitive strain fully rescued growth at 30 or 37°C, and most cells appeared normal morphologically, although a few cells with mutant morphology were present (unpublished data). Moreover, when YIp211-CDC3-GFP was used to replace the normal *CDC3* gene with *CDC3-GFP* (using the pop-in/pop-out technique; Rothstein, 1991), the resulting haploid strain grew at temperatures from 23 to 37°C (unpublished data). Cell morphologies appeared fully normal at 23 or 30°C; at 37°C, ~95% of the cells looked normal and ~5% had an elongated-bud morphology. Introduction of pRS315-GFP-BEM3 into the *bem3*Δ *rga1*Δ double-mutant strain YEF1035 partially rescued the cell-morphology phenotype, and pRS315-GFP-RGA1 produced a similar but more effective rescue (unpublished data).

To construct a plasmid expressing a GFP-tagged Myo1p, the *Not*I site in pRS316 was first filled in with Klenow polymerase to create pRS316-NoNot. Next, an ~7.3-kb *Cla*I-*Sal*I fragment was subcloned from YCp50-MYO1 (Vallen *et al.*, 2000) into *Cla*I/*Sal*I-digested pRS316-NoNot to create plasmid pRS316-MYO1. With this plasmid as template and the primers listed in Table 3, PCR was carried out to amplify the entire plasmid using the Expand Long-Template PCR system (Roche Diagnostics). The amplified DNA was digested with *Not*I and religated to create plasmid pRS316-N-*Not*I-MYO1, in which an in-frame *Not*I site had been introduced immediately after the *MYO1* start codon. Finally, a *Not*I *GFP*$^{F64L/S65T/V163A}$ cassette (Harkins *et al.*, 2001) was cloned into this *Not*I site to create plasmid pRS316-N-MYO1-GFP, which appeared to complement fully the cytokinesis and cell-separation defects of a *myo1*Δ strain (unpublished data).

Complete deletions of the *STE20*, *CLA4*, *SKM1*, and *RGA2* open reading frames were constructed using the PCR method (Baudin *et al.*, 1993; Longtine *et al.*, 1998b). A pair of hybrid primers (Table 3) was used to amplify *HIS3* (for

Table 2. Plasmids used in this study

Plasmid	Characteristics	Source
YEp13	High-copy (2 μm), *LEU2*	Rose and Broach (1990)
YEp24	High-copy (2 μm), *URA3*	Rose and Broach (1990)
YEplac181	High-copy (2 μm), *LEU2*	Gietz and Sugino (1988)
pRS316	Low-copy (CEN), *URA3*	Sikorski and Hieter (1989)
pRS315	Low-copy (*CEN*), *LEU2*	Sikorski and Hieter (1989)
pRS426	High-copy (2 μm), *URA3*	Christianson *et al.* (1992)
pPB547	*BEM3* in YEp13	Bi and Pringle (1996)
YEp13-RGA1	*RGA1* in YEp13	Bi and Pringle (1996)
YEp13-ZDS1*	*ZDS1* in YEp13	Bi and Pringle (1996)
YEp24-RGA1	*RGAI* in YEp24	Stevenson *et al.* (1995)
pDLB1981	*RGA2* in pRS426	Gladfelter *et al.* (2002)
YEp181-RGA1(WT)	*RGA1* in YEplac181	See text
YEp181-RGA1 (K872A)	$rgal^{K872A}$ in YEplac181	See text
pRS316-CDC3-GFP	*CDC3-GFP* in pRS316	See text
pRS316-N-MYO1-GFP	*MYO1-GFP* in pRS316	See text
YEp13-GFP-BEM3	*GFP-BEM3* in YEp13	See text
pRS315-GFP-RGA1	*GFP-RGA1* in pRS315	See text

STE20, *CLA4*, and *SKM1*) or *kanMX6* (for *RGA2*) from plasmid pRS303 (Sikorski and Hieter, 1989) or pFA6a-KanMX6 (Longtine *et al.*, 1998b). The amplified DNAs were transformed into strain YEF473 (for *STE20*, *CLA4*, and *SKM1*) or YEF982 (for *RGA2*) with selection for stable His^+ or $G418^R$ transformants. Tetrads were then dissected to obtain the haploid strains listed in Table 1. A strain heterozygous for an *RGA2-GFP* fusion was constructed similarly, using hybrid primers (Table 3) to amplify $GFP^{F64L/S65T}$ from plasmid pFA6a-GFP(F64L/S65T)-kanMX6 (I. Yu and J. Pringle, unpublished results) and transforming strain YEF473. The success of all deletion and tagging constructions was confirmed by PCR using the primers listed in Table 3.

Microscopy

Cells were observed either without fixation or after fixation by adding formaldehyde directly to the growth medium to a final concentration of 3.7%. Overall cell morphologies were observed by differential interference contrast (DIC) microscopy, and indirect immunofluorescence was performed as described by Pringle *et al.* (1991). Cdc11p was visualized using rabbit polyclonal antibodies (Ford and Pringle, 1991). HA-tagged proteins were visualized using mouse monoclonal anti-HA-epitope antibody (HA.11; Berkeley Antibody Company, Richmond, CA) at 1:100 dilution. FITC-conjugated goat anti-rabbit IgG and donkey anti-mouse IgG secondary antibodies were purchased from Jackson ImmunoResearch (West Grove, PA) and used at 1:200 dilution. DNA was stained with 1 μg/ml bisBenzimide (Sigma, St. Louis, MO).

For time-lapse microscopy, cells growing exponentially in liquid SC-Ura medium were spotted onto a microscope slide spread with a thin layer of SC-Ura medium solidified with 25% gelatin (Yeh *et al.*, 1995). Individual cells were followed at 15-min intervals using a computer-controlled microscope (Eclipse E800; Nikon, Tokyo, Japan) with motorized focus and a high-resolution CCD camera (model C4742–95; Hamamatsu Photonics, Bridgewater, NJ). For each time point, one DIC image (exposure time: 0.6 s) and three GFP images (exposure times: 2–3 s each, with a stage increment of 1.2 μm) were acquired and analyzed using Image-Pro Plus software (Media Cybernetics, Silver Spring, MD). The contrast of the images was enhanced using Image-ProPlus and/or Adobe PhotoShop Version 4.0 (Adobe Systems, San Jose, CA).

FRAP studies of Cdc3p-GFP were performed using a Zeiss laser scanning confocal microscope with LSM510 Software Version 2.5 (Zeiss, Thornwood, NY). Excitation for image acquisition (λ = 488 nm) was set at 4–5% of the maximal laser intensity. Recovery of fluorescence was monitored after bleaching with 10 iterations (over a total of 2.1 s) of 100% laser intensity at 488 nm. In each FRAP series, images of the cells were captured before and immediately after bleaching, and the recovery phase was followed at intervals of 2 min for up to 16 min. For representative series, the cells were aligned, and the fluorescence intensity at each time point was quantitated using Metamorph Version 4.0 software (Universal Imaging, Downingtown, PA) and plotted against time. Each value on the *y*-axis represents the ratio of the fluorescence intensity of the bleached or unbleached portion of the tested septin structure (minus the background fluorescence intensity) to the fluorescence intensity of the unbleached septin structure from a control cell in the same field (minus the background fluorescence intensity) at the same time point. Because the control cells were selected to have small- or medium-sized buds (and thus to have stable septin rings; see Figure 8), determining these ratios controls for photobleaching during image acquisition in the course of the experiment.

RESULTS

Suppression of Septin Defects by Increased Dosage of Cdc42p GAPs

We reported previously that multicopy *BEM3* or *RGA1* exacerbated the phenotypes (i.e., decreased the restrictive temperatures) of *cdc24-ts* and *cdc42-ts* strains (Stevenson *et al.*, 1995; Bi and Pringle, 1996). This result was expected, because increased dosage of a Cdc42p GAP would presumably decrease the amount of active, GTP-bound Cdc42p in the cell. In the same studies, we used a Ts^- septin strain (*cdc12-6*) as a control. Surprisingly, multicopy *BEM3* or *RGA1* suppressed the defects of this strain both in cell growth (Pringle *et al.*, 1995; Figure 1A) and in cell morphology (Figures 1B and 2B, middle panel). *RGA2*, which encodes a third Cdc42p-GAP, also weakly suppressed the *cdc12-6* growth defect (Figure 1A). Multicopy *BEM3* or *RGA1* also suppressed the *cdc12-5* and *cdc10-1* septin mutations at 30°C, but they failed to suppress two other Ts^- septin mutations, *cdc3-3* and *cdc11-6*, at temperatures from 30 to 37°C (unpublished data). The suppression by *RGA1* was relatively strong and consistent, whereas the suppression by *BEM3* was weaker and more variable from experiment to experiment (perhaps reflecting variations in plasmid copy number).

We also examined septin organization in the *cdc12-6* strains. When a strain carrying vector alone was incubated at 30°C, a functional GFP-Cdc3p localized to the tips of the elongated buds or formed abnormal-looking structures at the mother-bud neck in most cells (Figures 1C, left panel, and 2C, top panel). In contrast, in a strain carrying multicopy *RGA1*, the GFP-Cdc3p localized to a normal-looking ring at the mother-bud neck in most cells, including those with very small buds (Figures 1C, right panel, and 2C, middle panel). As judged by the same assay, the suppression of septin-organization defects by multicopy *BEM3* was variable (unpublished data). Taken together, the data suggest that the suppression of septin defects by increased dosage of Rga1p (or, less effectively, of Bem3p or Rga2p) involves a promotion of septin-ring formation at the neck. The data also suggest that under some conditions, complete or partial inactivation of one septin can lead not to complete disper-

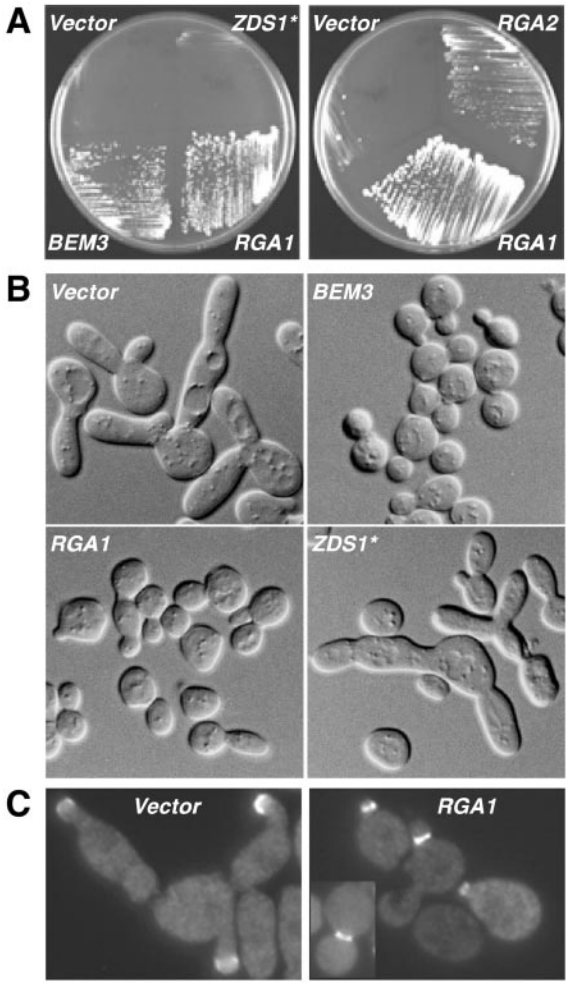

Figure 1. Suppression of the growth, morphological, and septin-organization defects of a *cdc12-6* mutant by multicopy *BEM3*, *RGA1*, or *RGA2*. *ZDS1*, a putative non-GAP negative regulator of Cdc42p (Bi and Pringle, 1996), was included as a negative control. (A) Strain M-17 (*cdc12-6*) was transformed (left panel) with plasmid YEp13 (vector), pPB547 (*BEM3* in YEp13), YEp13-RGA1, or YEp13-ZDS1* and (right panel) with plasmid YEp24 (vector), YEp24-RGA1, or pDLB1981 (*RGA2* in pRS426). The transformants were streaked and incubated at 30°C on an SC-Leu plate for 3 d (left panel) or an SC-Ura plate for 5 d (right panel). (B) The transformants in A (left panel) were grown to exponential phase in liquid SC-Leu medium at 23°C, diluted 1:10 in prewarmed medium, and incubated at 30°C for 3.4 h. Cells were then sonicated mildly and observed by DIC microscopy. Each image is printed at the same magnification. (C) Strain M-17 carrying plasmid pRS316-CDC3-GFP was further transformed with plasmid YEp13 (left) or YEp13-RGA1 (right). The transformants were grown to exponential phase in liquid SC-Leu-Ura medium at 23°C, shifted to 30°C for 3 h, fixed with 3.7% formaldehyde for 20 min (10 min at 30°C and 10 min at 23°C), and observed by fluorescence microscopy. The images are printed at the same magnification.

sion of the other septins in the cytoplasm but to their formation of abnormal structures at the bud tip or neck.

To ask if the suppression of septin defects by *RGA1* requires the interaction of Rga1p with Cdc42p, we used a mutant *RGA1* in which the conserved Lys-872 is replaced by Ala. As observed also with mammalian Rho-GAPs (Li *et al.*, 1997), this change drastically decreases both the interaction between Rga1p and Cdc42p and Rga1p GAP activity (Gladfelter *et al.*, 2002). In our genetic assay, multicopy *rga1*^{K872A} failed to suppress the defects of *cdc12-6* in cell growth (Figure 2A), overall cell morphology (Figure 2B), and septin organization (Figure 2C).

Defective Septin Organization in Cdc42p GAP Mutants

If the Cdc42p GAPs positively regulate septin-ring formation, deletion of the GAP genes might lead to a septin defect. To test this possibility, we deleted *BEM3*, *RGA1*, and *RGA2* either singly or in combination and examined the resulting cell morphologies and septin structures. None of the single mutants showed any readily detectable defects (unpublished data), but the double and triple mutants showed variably severe defects that resembled those of septin mutants. The *bem3*Δ *rga2*Δ and *rga1*Δ *rga2*Δ double mutants had only mild defects (unpublished data), but the *bem3*Δ *rga1*Δ double mutant and the triple mutant had pronounced defects in both cell morphology (Figure 3A) and septin organization; in the triple mutant, the majority of cells showed such abnormalities. Instead of the normal ring structure at the mother-bud neck (Figure 3B, left panel), the septins often formed parallel bars in the neck (Figure 3, B and C, arrowheads) or a cap on the bud (Figure 3, B and C, arrows). This disorganization of the septins was paralleled by disorganization of the type II myosin Myo1p, a contractile-ring component that normally localizes to the mother-bud neck throughout the cell cycle in a septin-dependent manner (Bi *et al.*, 1998; Lippincott and Li, 1998; Figure 4A). In many *bem3*Δ *rga1*Δ *rga2*Δ cells, Myo1p formed a ring that looked normal or nearly so (Figure 4B, cells 1 and 2). However, in nearly all of the cells that had severely elongated buds, Myo1p formed abnormal structures, including patches in the neck region and cables in the cytoplasm (Figure 4B, cell 3). Although even the triple GAP mutant was viable and sometimes showed seemingly normal organization of the septins and associated proteins, the abnormalities observed in many other cells support the hypothesis that the Cdc42p GAPs play a role in formation of the normal septin ring.

To explore this role further, we constructed strains carrying both the GAP deletions and other mutations that affect septin organization. Mutation of the PAK-kinase gene *CLA4* produces significant defects in septin organization and cell morphology (Cvrcková *et al.*, 1995; Richman *et al.*, 1999; Longtine *et al.*, 2000; Weiss *et al.*, 2000; Figure 5A). However, a *bem3*Δ *rga1*Δ *cla4*Δ triple mutant had defects in both cell morphology (Figure 5A) and septin organization (Figure 5B) that were much more severe than those of either the *cla4*Δ single mutant or the *bem3*Δ *rga1*Δ double mutant (cf. Figure 3, A and B). In contrast, deletion of either of the other PAK-kinase genes, *STE20* and *SKM1*, did not significantly exacerbate the phenotype of a *bem3*Δ *rga1*Δ strain (Figure 5A). These results suggest that Cla4p and the Cdc42p GAPs have complementary functions that promote normal septin organization.

An even more dramatic effect was seen when the GAP deletions were combined with deletion of the protein kinase gene *GIN4*. Deletion of *GIN4* alone produces significant but relatively mild effects on growth, cell morphology, and septin organization (Longtine *et al.*, 1998a; Figure 5, C–E). However, the *bem3*Δ *rga1*Δ *gin4*Δ triple mutant was nearly dead (Figure 5C). The mutant cells produced grossly elongated buds (Figure 5, D and F) in which the nuclear cycle continued (Figure 5G). This phenotype is very similar to that associated with a complete loss of septin function (Hartwell, 1971; Adams and Pringle, 1984; Longtine *et al.*, 1996), and

Table 3. Primers used for gene deletion and tagging

Name of primer	Sequence of primer
Primers used for PCR-mediated deletions and tagging[a]	
STE20 Del-forward	CATCCTAAATATCCCACAAGATCCTCGACTAATACAAGAAGATTGTACTGAGAGTGCAAC
STE20 Del-reverse	TATACTTTGTCGATAATAAGGTGTACCCTGCTTGCTACGTCTGTGCGGTATTTCACACCG
STE20 Del-check-forward	GAAAGCACTGATCCATCAATTAAAGCACCGAAC
SKM1 Del-forward	TACTCGAGGACAATCAGACAAAACGAAAGAATATCTTTCGATTGTACTGAGAGTGCACC
SKM1 Del-reverse	ATATATATATTGTTTCTCCTAAATAAAAAAAAAGCTAAATTCTGTGCGGTATTTCACACCG
SKM1 Del-check-forward	ACCGTATACGCTTGATTTCGTCAG
RGA2 Del-forward	CGTAGCATCTCAAGAGCAAGGAGATTTTGATGAAAAAAATCGGATCCCCGGGTTAATTAA
RGA2 Tag-forward	ATTTATACTTGGAAACTATAGAGACATATTTAAGCAAGCACGGATCCCCGGGTTAATTAA
RGA2 Del/Tag-reverse	TTAATCTATCCTATGTTTATTTAACTTTTGCAAATCTGTAGAATTCGAGCTCGTTTAAAC
RGA2 Del/Tag-check-reverse	TCTTTTACCCTTTTGCTGTTTTCC
Mutagenic primers used to introduce *Not*I sites[b]	
BEM3-*Not*I	AACTAACAGCACGCAATGAGCGGCCGCACAGATAATTTGACCACA
RGA1-*Not*I	GAGCGGCATATTAAAATGAGCGGCCGCGCATCAACTGCTCCCAAT
CDC3-*Not*I	GTGTCCATTAAGCAGGACCCGGGCGGCCGCGAAGAGCGT
MYO1-N-*Not*I-forward	ATGAGCGGCCGCACCGGCGGGCAGTCTTGCAGTTCTAATATG
MYO1-N-*Not*I-reverse	GGTGCGGCCGCTCATTATTGCTGTTGTTGTCCTGTCTAACTTTG

[a] The underlined sequences correspond to those immediately upstream or downstream of the coding region to be deleted or immediately upstream of the stop codon of the gene to be tagged. The primers used to delete *CLA4* have been described by Longtine *et al.* (2000).
[b] The *Not*I sites are underlined.

septin organization was indeed severely abnormal in nearly all of the triple-mutant cells (Figure 5, E–G). Similarly, Myo1p organization was also grossly abnormal in the *bem3*Δ *rga1*Δ *gin4*Δ triple mutant (Figure 4C). Thus, Gin4p and the Cdc42p GAPs appear to play critical and complementary roles in promoting normal septin organization.

The cell-morphology and septin-organization defects in the *bem3*Δ *rga1*Δ *rga2*Δ and *bem3*Δ *rga1*Δ *gin4*Δ triple mutants were only partially suppressed (indeed, hardly at all in the case of the *bem3*Δ *rga1*Δ *gin4*Δ strain) by deletion of *SWE1* (unpublished data). As Swe1p is an essential component of the morphogenesis checkpoint that causes a G2 delay in response to morphogenetic defects (Lew and Reed, 1995; Barral *et al.*, 1999; Shulewitz *et al.*, 1999; Longtine *et al.*, 2000), the phenotypes of the triple mutants must not result primarily from activation of this checkpoint.

Septin-Organization Defects in a cdc42 Mutant

In another line of experiments, random PCR-generated mutations in *CDC42* were screened to identify alleles that cause distinct changes in cell morphology (Caviston *et al.*, 2002). One temperature-sensitive allele, *cdc42-76*, is described further here. Even at a temperature permissive for growth (23°C), *cdc42-76* cells grew more slowly than an isogenic wild-type strain (unpublished data) and were uniformly elongated (Figure 6A), resembling a septin mutant. Indeed, septin organization was altered drastically in the mutant cells (Figure 6B). The defects were similar to, but significantly more severe than, those displayed by the triple GAP mutant and included septin caps on buds (Figure 6B, arrowheads) and septin bars or patches in the necks or in the cortex of the elongated buds. At 37°C, *cdc42-76* cells arrested growth with a slightly elongated cell morphology (unpublished data). Sequencing showed that this allele contains two codon changes, GTG to GGG at codon 36 (V36G) and TCT to TCA at codon 89 (S89S). Although it is conceivable that a change in translation efficiency at codon 89 contributes to the mutant phenotype, we will henceforth refer to *cdc42-76* as $cdc42^{V36G}$. Other mutations at residue 36 (V36T and V36A) also cause relatively specific defects in septin organization (Kozminski *et al.*, 2000; Gladfelter *et al.*, 2001a, 2002). However, $cdc42^{V36G}$ is significantly more penetrant in its phenotype (at least in our strain background) and thus strengthens the evidence for a specific role of Cdc42p in promoting normal septin assembly. It also provides a useful tool for further studies, as described below.

Localization of Cdc42p GAPs in the Cell Cycle

Cdc42p is localized to the presumptive bud site early in the cell cycle (Ziman *et al.*, 1993; Richman *et al.*, 2002) and controls the initial formation of the septin ring at that stage. Cdc42p is also localized to the mother-bud neck late in the cell cycle (Richman *et al.*, 2002) and thus might play an additional role in maintaining septin organization (or promoting reorganization) at that stage. Thus, the Cdc42p GAPs might promote proper septin organization at either or both of these stages. To explore these possibilities, we used tagged proteins (see MATERIALS AND METHODS) to localize the GAPs during the cell cycle. When either 3HA-Bem3p or Rga2p-GFP was expressed from a chromosomal copy of the gene under the control of its normal promoter, the localization signals were weak but unambiguous. Like Cdc42p itself, both GAPs were observed to be localized to presumptive bud sites, the tips of small buds, and the necks of cells late in the cell cycle, although no distinct signal could be detected at intermediate stages (Figure 7, A and D). When GFP-Bem3p was expressed from a high-copy plasmid, the localization signals were stronger but otherwise similar (Figure 7B), except that the Bem3p in the neck of large-budded cells appeared to be conterminous with the entire, hourglass-shaped septin ring rather than forming a narrower ring near the middle of the neck (cf. Figure 7A).

When GFP-Rga1p was expressed from a low-copy plasmid or 3HA-Rga1p was expressed from an integrated single

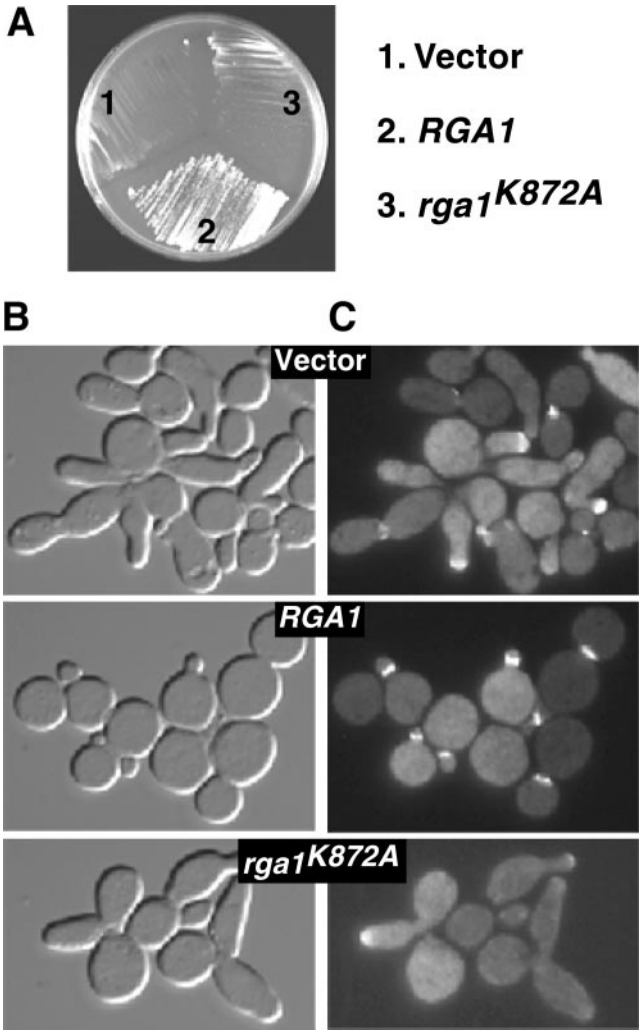

Figure 2. Dependence of *cdc12* suppression on the interaction of Rga1p with Cdc42p and/or its GAP activity. Strain M-17 (*cdc12-6*) was transformed with plasmid YEplac181 (Vector), YEp181-RGA1(WT) (*RGA1*), or YEp181-RGA1(K872A) ($rga1^{K872A}$). (A) The transformants were streaked onto a SC-Leu plate and incubated at 30°C for 5 d. (B and C) The transformants were further transformed with plasmid pRS316-CDC3-GFP, grown to exponential phase in liquid SC-Leu-Ura medium at 23°C, and shifted to 30°C for 3 h before fixation (as in Figure 1C) and examination by DIC (B) and fluorescence (C) microscopy.

copy of the gene under the normal *RGA1* promoter, the localization observed was somewhat different from that of the other GAPs and from that of Cdc42p itself. Rga1p was also localized to presumptive bud sites (Figure 7E, cell 1) and to small buds, but in the latter, it seemed to be present throughout the bud cortex rather than only at the bud tip (Figure 7E, cell 2). Moreover, in cells with somewhat larger buds (a stage at which polarized localization of Cdc42p [Richman *et al.*, 2002], Bem3p, and Rga2p was not detectable; see above), Rga1p appeared as a ring at the neck that was asymmetrically localized to the bud side (Figure 7E, cell 3, and unpublished data). Later in the cell cycle, the ring of Rga1p at the neck appeared more symmetric and was conterminous with the entire septin ring (Figure 7E, cell 4, and 7F).

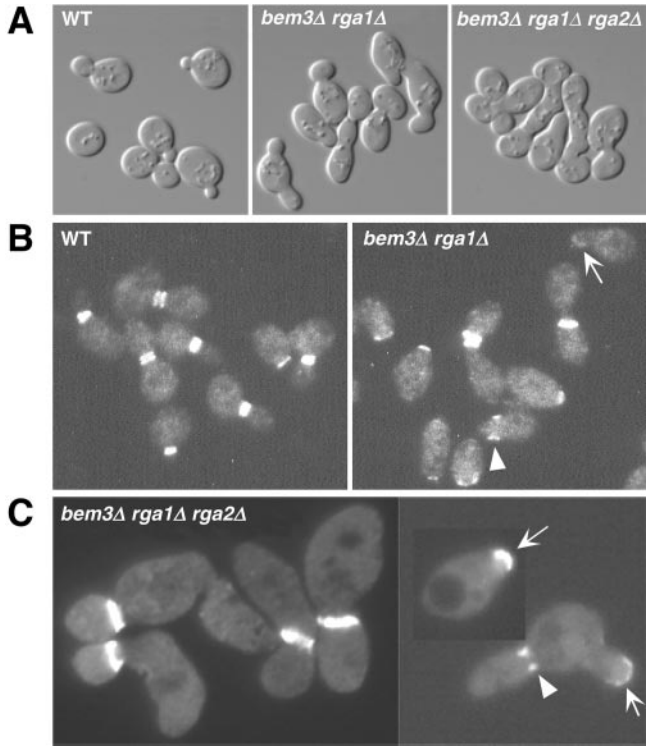

Figure 3. Cell-morphology and septin-organization defects in strains lacking Cdc42p GAPs. (A and B) Wild-type (WT) strain YEF473A, *bem3*Δ *rga1*Δ strains YEF2390 (A) and YEF1209 (B), and *bem3*Δ *rga1*Δ *rga2*Δ strain YEF2335 were grown to exponential phase in liquid YM-P (A) or YPD (B) medium at 23°C and then observed by DIC microscopy (A) or processed for immunofluorescence using Cdc11p-specific antibodies (B). (C) *bem3*Δ *rga1*Δ *rga2*Δ strain YEF2380 was transformed with plasmid pRS316-CDC3-GFP, grown overnight on an SC-Ura plate at 24°C, and examined by fluorescence microscopy.

To ask if the localization of the Cdc42p GAPs depends on the septins, we expressed tagged Bem3p or Rga1p in a temperature-sensitive septin mutant. On shift to restrictive temperature, septin structures were lost from the neck (Figure 7G, middle panel), and the GAPs were no longer detectable at the necks of large-budded cells (Figure 7C, bottom cell, and 7G, top panel). Wild-type cells subjected to the same temperature shift showed no loss of GAP localization from the neck (unpublished data), and the GAPs remained detectable in the mutant at presumptive bud sites and the tips of small and elongating buds (Figure 7C, top three cells, and 7G, top panel). Thus, localization of the Cdc42p GAPs to the neck, but not to the presumptive bud site or bud tip, depends on the septins. Taken together, these data support the hypothesis that the Cdc42p GAPs play a role in organizing the septins at the beginning of the cell cycle, whereas the neck localization of the GAPs may reflect a septin-dependent role in other cellular processes.

Cell Cycle–regulated Septin Dynamics

To explore further the factors controlling septin organization, we examined the dynamics of septin structures using FRAP on cells expressing a functional GFP-tagged Cdc3p. We first examined the septin structures seen at different stages of the wild-type cell cycle (see INTRODUCTION).

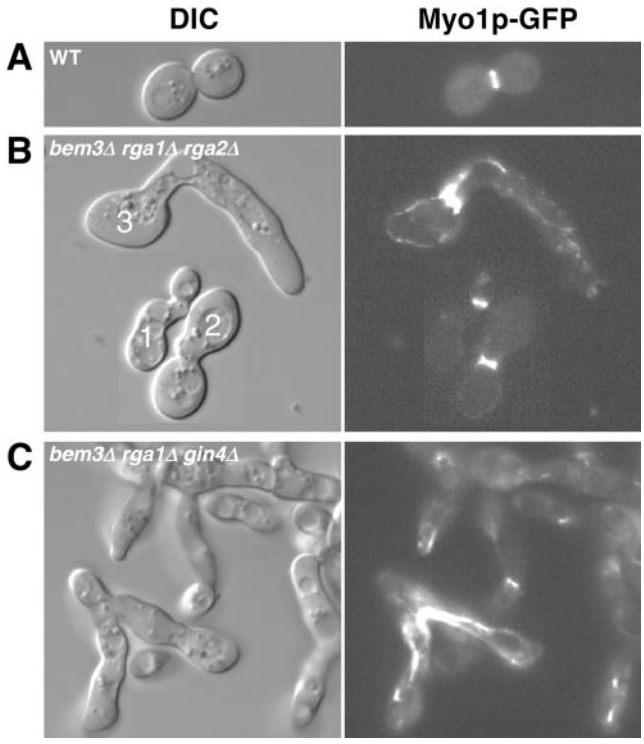

Figure 4. Disorganization of Myo1p in strains lacking Cdc42p GAPs. Wild-type strain YEF473A (A), *bem3*Δ *rga1*Δ *rga2*Δ strain YEF2380 (B), and *bem3*Δ *rga1*Δ *gin4*Δ strain YEF2517 (C) were transformed with plasmid pRS316-N-MYO1-GFP, grown on SC-Ura plates for ~36 h at 23°C, and examined for cell morphology and Myo1p localization by DIC (left) and fluorescence (right) microscopy.

When the septin rings on unbudded cells were bleached, the recovery of fluorescence was rapid (Figure 8A). The "total-bleached" rings recovered as well as did the "half-bleached" rings, indicating that recovery involves recruitment of fluorescent subunits from an unassembled pool and not simply lateral mobility within the existing structure. Rapid recovery would, of course, be expected in cells that were bleached during the period in which the septin ring was still in the process of forming. However, all 19 unbudded cells examined behaved similarly, suggesting that the dynamic state of the septin ring persists after it appears to be fully formed and at least until the bud emerges.

In contrast, when the septin rings of cells with small or medium-sized buds were bleached, there was little recovery of fluorescence by either half-bleached or total-bleached rings (Figure 8B). Thus, the extension of the initial septin ring into the hourglass-shaped structure as the bud emerges appears to be accompanied by a change in septin organization such that the structure is more stable and has neither substantial lateral mobility of subunits within the structure nor substantial exchange of subunits with any unassembled pool.

At the end of the cell cycle, when the septin ring splits and then begins to disassemble, it again appears to become dynamic and capable of rapid subunit exchange, because the bleached portions of half-bleached rings showed rapid, partial recovery of fluorescence even as the unbleached portions of the same rings showed a gradual decrease in fluorescence (Figure 8C). (Note that because of the normalization procedure used, this decrease must be due to disassembly rather than simply to photobleaching during image acquisition.) Interestingly, at this stage, total-bleached rings showed significantly poorer recovery than did the bleached portions of half-bleached rings (Figure 8C and unpublished data). This suggests that there may be few unassembled fluorescent subunits at this stage, so that the recovery of fluorescence in the bleached portions of half-bleached rings may result in part from exchange with subunits that are being released by disassembly of the unbleached portions of the same rings.

Finally, we also examined the dynamics of the septin structures that form in the *cdc42*^{V36G} and triple Cdc42p-GAP mutants (see Figures 3 and 6). Most of the abnormal caps and patches appeared to be highly dynamic, because they showed rapid and extensive recovery of fluorescence after bleaching (Figure 8D). In contrast, bleaching the relatively normal-looking septin rings found in many of the mutant cells revealed a range of behaviors. Among 14 rings that resembled those on wild-type cells with small or medium-sized buds, only two recovered fluorescence quickly, whereas 6 showed very little recovery and 6 gave intermediate results (unpublished data). Taken together with the data on wild-type cells, the observations on the mutant cells suggest that Cdc42p and its GAPs are important for the structural transition by which the dynamic septin ring of the unbudded cell becomes the more stable ring of the budded cell.

Relationship between Septin Organization and Cell Morphology

The variability and lability of the septin structures in the *cdc42*^{V36G} and triple Cdc42p-GAP mutant cells allowed us to examine the transition from abnormal to relatively normal septin structure and to establish an interesting correlation between the pattern of septin organization and the pattern of bud growth. Time-lapse observations on cells expressing Cdc3p-GFP showed that in the mutants, many emerging and small buds had septin caps on the buds (Figure 9, A and B, 0 min). These caps persisted for varying times on different cells, but so long as they were present, the buds invariably ($n = 26$) grew with an abnormally elongated shape and lacked a clear neck-like constriction (Figure 9B, 60–120 min). In 15 of these 26 cells, the septin cap was transformed into a structure resembling a normal septin ring at some point during the time-lapse observations of bud growth (Figure 9A, compare 0 to 45 min, and 9B, compare 120 to 150 min). Immediately after this transformation, in every case, a bud of more normal shape began to form distal to the septin ring, with a clear neck-like constriction at the site of the ring (Figure 9A, 45–90 min, and 9B, 150–195 min). These buds then continued to grow and eventually underwent cytokinesis and cell separation at the site of the septin ring, seemingly as in wild-type cells (unpublished data). Consistent with the FRAP results, these observations suggest that the *cdc42*^{V36G} defect or the loss of Cdc42p-GAP activity impedes, but does not wholly prevent, the transformation of a labile precursor structure into a stable septin ring, which can then function relatively normally. The observations also suggest that the presence of a properly organized septin ring is necessary for the growth of a bud of normal shape.

DISCUSSION

Promotion of Septin-ring Formation by the Cdc42p GAPs

In this study, we have presented several lines of evidence suggesting that the Cdc42p GAPs Bem3p, Rga1p, and Rga2p play a positive role(s) in generating normal septin organiza-

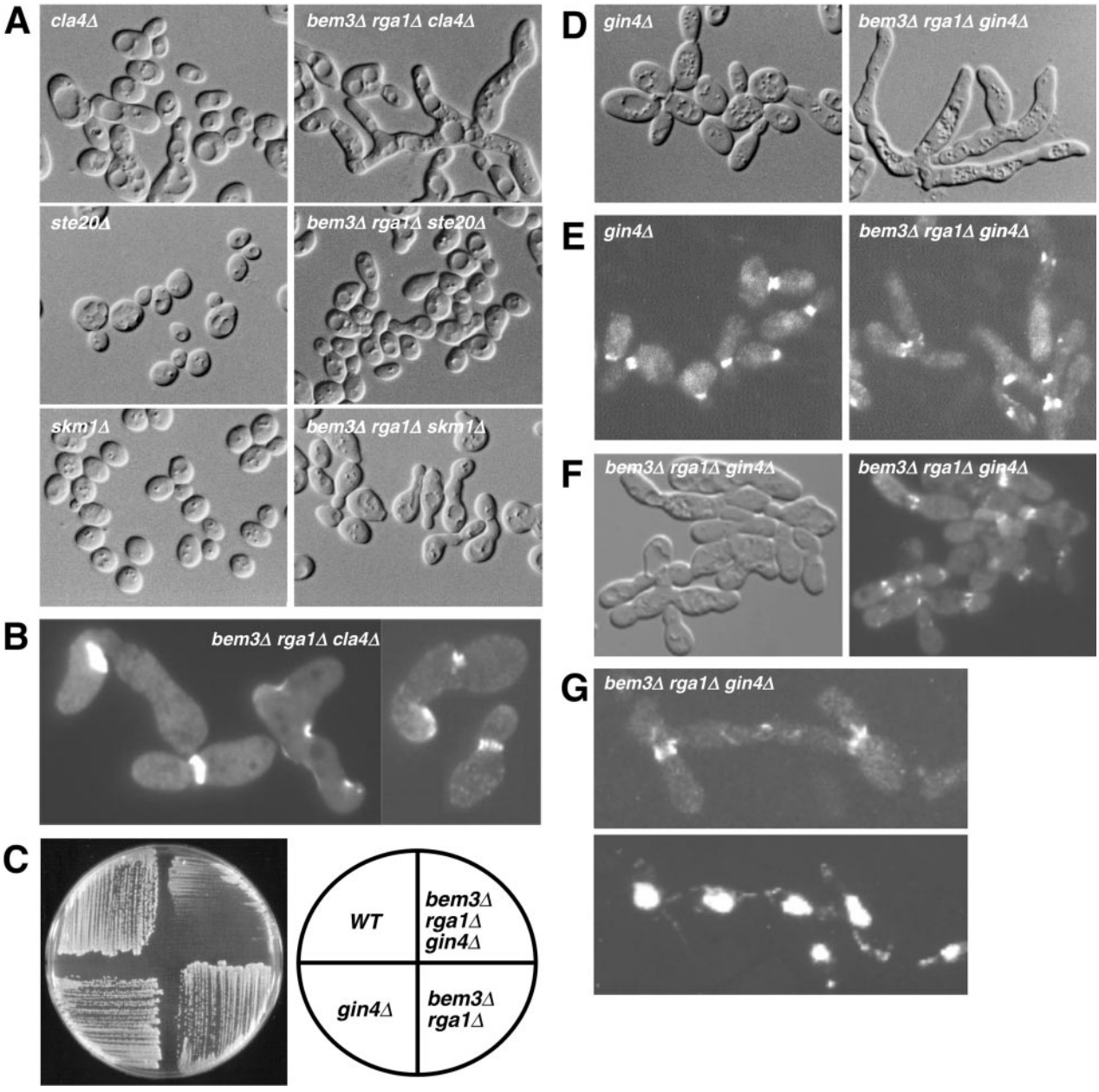

Figure 5. Synthetic effects between Cdc42p-GAP mutations and mutations in protein kinases involved in septin organization. (A) Strains YEF1343 (*cla4*Δ), YEF1383 (*bem3*Δ *rga1*Δ *cla4*Δ), YEF1341 (*ste20*Δ), YEF1381 (*bem3*Δ *rga1*Δ *ste20*Δ), YEF1347 (*skm1*Δ), and YEF1385 (*bem3*Δ *rga1*Δ *skm1*Δ) were observed by DIC microscopy after overnight growth on YPD plates at 23°C. (B) Strain YEF1383 was transformed with plasmid pRS316-CDC3-GFP and observed by fluorescence microscopy after overnight growth on an SC-Ura plate at 24°C. (C) Strains YEF473A (WT), M-267 (*gin4*Δ), YEF1209 (*bem3*Δ *rga1*Δ), and YEF1300 (*bem3*Δ *rga1*Δ *gin4*Δ) were picked from a YPD plate containing 0.9 M KCl (which partially suppresses the *gin4*Δ mutant phenotype; our unpublished results), streaked onto a YPD plate, and incubated at 23°C for ~2.5 d. (D) Strains M-267 and YEF1300 were streaked from YPD + 0.9 M KCl plates onto YPD plates, grown overnight at 23°C, and observed by DIC microscopy. (E) Strains M-267 and YEF1300 were grown overnight in liquid YPD + 0.9 M KCl at 23°C, collected by centrifugation, washed twice with liquid YPD medium, diluted 1:50 with fresh YPD, grown for 9 h at 23°C, and processed for immunofluorescence using Cdc11p-specific antibodies. (F) Strain YEF2517 (*bem3*Δ *rga1*Δ *gin4*Δ) was transformed with plasmid pRS316-CDC3-GFP, grown overnight in liquid SC-Ura medium at 23°C, fixed with 3.7% formaldehyde for 10 min at 23°C, and examined by DIC (left) and fluorescence (right) microscopy. (G) Strain YEF1300 was grown as described for panel E and double-stained with anti-Cdc11p antibodies (top) and bisBenzimide to visualize the DNA (bottom).

tion. First, overexpression of the GAPs could suppress the growth, morphology, and septin-organization defects of some temperature-sensitive septin mutants (Figure 1). This suppression contrasted sharply with the exacerbation of *cdc24* or *cdc42* temperature-sensitive phenotypes by overexpression of the GAPs and with the lack of suppression of the septin defects by overexpression of Zds1p, a putative non-GAP negative regulator of Cdc42p (Figure 1; Stevenson *et al.*,

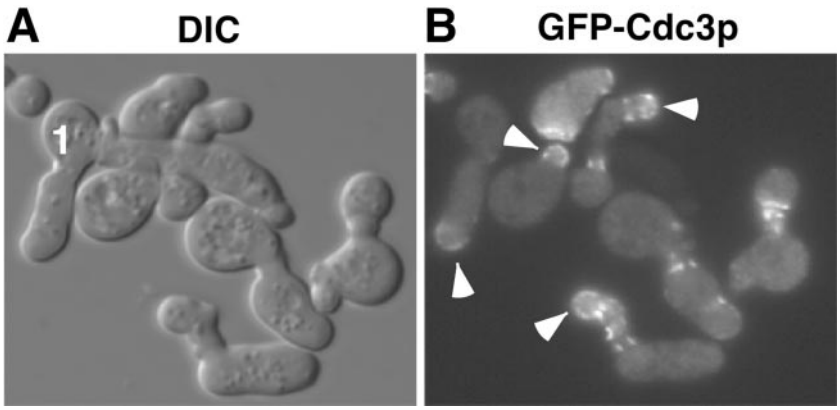

Figure 6. Cell-morphology and septin-organization defects in $cdc42^{V36G}$ cells. Cells of strain YEF2921 ($cdc42^{V36G}$) carrying plasmid pRS316-CDC3-GFP were grown to exponential phase in liquid SC-Ura medium at 23°C, fixed with 3.7% formaldehyde for 10 min at 23°C, and examined by DIC (A) and fluorescence (B) microscopy. Arrowheads indicate septin caps. Note that the longer bud of cell 1 (A) is out of the plane of focus in B.

1995; Bi and Pringle, 1996). Second, mutants lacking the GAPs had defects in the organization of the septins and of proteins whose localization depends upon the septins, and hence in cell morphology (Figures 3 and 4). In GAP mutants that also lacked Cla4p or Gin4p, two other proteins known to promote normal septin organization (Cvrcková *et al.*, 1995; Longtine *et al.*, 1998a, 2000; Weiss *et al.*, 2000), these defects were strongly exacerbated (Figures 4 and 5). Finally, each of the three GAPs colocalizes with the septins both around the time of bud emergence and around the time of cytokinesis (Figure 7).

Data consistent with ours have also been reported recently by others (Gladfelter *et al.*, 2001, 2002; Smith *et al.*, 2002). Although there are some differences in the details (perhaps due to differences in strain backgrounds), both groups also observed septin-organization and cell-morphology defects in mutants lacking GAPs, and Smith *et al.* (2002) also observed synthetic growth defects between *cla4* and *rga1* or *rga2* mutations. In addition, Gladfelter *et al.* (2001, 2002) observed that the $cdc42^{V36T}$ and $cdc42^{Y32H}$ mutations, like the $cdc42^{V36G}$ mutation described here (Figure 6), specifically affected septin (rather than actin) organization and that these mutations could be suppressed by overexpression of Rga1p.

An important question is when in the cell cycle the GAPs play their putative role(s) in promoting normal septin organization and function. Multiple lines of evidence suggest that this occurs primarily or exclusively during the initial formation of the septin ring around the time of bud emergence. First, overexpression of Rga1p (and, more variably, of Bem3p) could restore the formation of normal-looking septin rings, even in small-budded cells, in a septin mutant that could rarely form them in the absence of such overexpression (Figure 1C). Second, in the *bem3 rga1* and *bem3 rga1 rga2* mutants (and even more dramatically in the *bem3 rga1 cla4* and *bem3 rga1 gin4* mutants), many cells appeared not to form normal septin rings in the first place (as opposed to forming normal rings that later became disorganized). Third, because *cla4* and *gin4* mutations appear to affect the initial formation of the septin ring (Cvrcková *et al.*, 1995; Longtine *et al.*, 1998a, 2000; Weiss *et al.*, 2000), the synthetic effects between these mutations and the GAP mutations suggest that the GAPs also affect septin organization at this stage. Fourth, when $cdc42^{V36G}$ or GAP mutant cells that had initially failed to form septin rings did so later after a period of abnormal bud growth, the rings that formed looked normal and appeared to behave normally during subsequent bud growth and cytokinesis (Figure 9 and unpublished data). Fifth, Gladfelter *et al.* (2002) presented good evidence that in G2 cells, continued Cdc24p and Cdc42p function (and thus, presumably, also continued Cdc42p-GAP function) is not needed for the maintenance of septin organization. Finally, we observed that localization of the GAPs to the necks of cells late in the cell cycle depends on the septins, although their localization to the presumptive bud site does not (Figure 7). These observations suggest that the GAPs function upstream of the septins in the initial organization of the bud site, whereas the later localization of the GAPs and of Cdc42p itself to the neck reflects the usual septin role in recruiting other proteins to the neck for various purposes.

A Two-step Model for Septin-ring Formation

Several lines of evidence suggest that the formation of the septin ring is a process that involves at least two distinguishable steps, which we refer to as "recruitment" (the delivery of septin monomers or oligomers to the appropriate site in the cell cortex) and "assembly" (the generation of the higher-order organization that characterizes the mature, hourglass-shaped septin ring of the budded cell; Figure 10A). First, the FRAP data show a clear transition between the relatively labile septin structures present before bud emergence and the more stable (less exchangeable) structures present in budded cells (Figure 8). Despite some differences in the details of their results, Dobbelaere *et al.* (2003) have recently reached the same conclusion from independent FRAP experiments. Second, in a variety of mutants (certain *cdc42* mutants, Cdc42p GAP mutants, and *cla4, gin4, bni5, nap1,* and *elm1* mutants), the septins appear to be recruited to an appropriate site in the cell cortex but fail to form a normal structure there; the caps, patches, and bars that do form differ both in appearance and in their continuing lability (as judged by FRAP) from normal septin rings (Figures 3, 5, 6, 8, and 9; Cvrcková *et al.*, 1995; Longtine *et al.*, 1998a, 2000; Sreenivasan and Kellogg, 1999; Weiss *et al.*, 2000; Bouquin *et al.*, 2000; Gladfelter *et al.*, 2001, 2002; Lee *et al.*, 2002; Smith *et al.*, 2002; Dobbelaere *et al.*, 2003). These observations suggest that Cdc42p itself, the Cdc42p GAPs, Cla4p, Gin4p, Bni5p, Nap1p, and Elm1p are all involved in a distinct assembly step (or steps; see below) that follows the initial Cdc42p-dependent recruitment of the septins to the presumptive bud site. Finally, in EM studies (Byers and Goetsch, 1976a; Byers, 1981), it appeared that the septin-associated "neck filaments" were not fully developed until a short time after bud emergence. In contrast, fluorescence studies have shown that the septins are concentrated at the presumptive bud site ~10 min before bud emergence (Kim *et al.*, 1991;

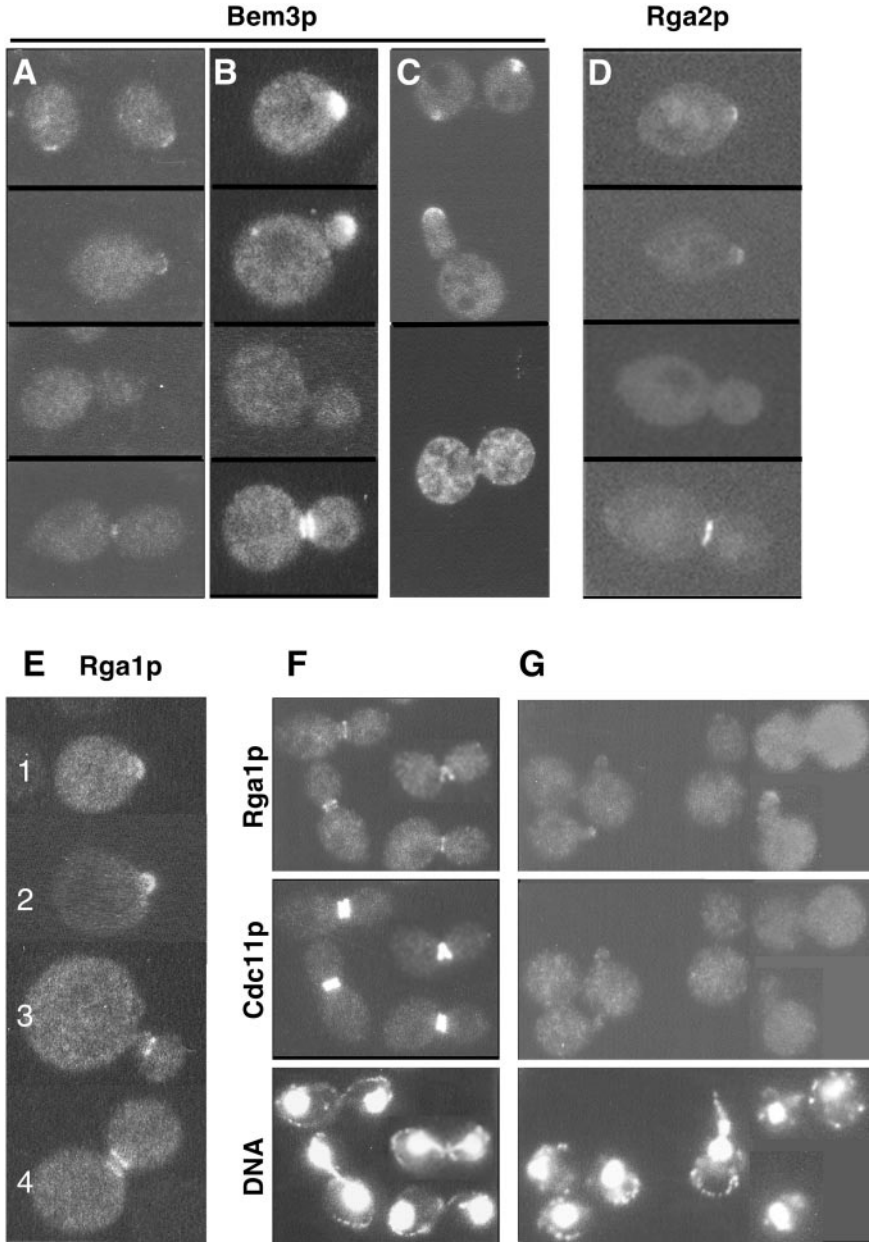

Figure 7. Localization of Cdc42p GAPs. (A–C) Localization of Bem3p and its dependence on septin function. (A) Strain YEF1423 (*3HA:BEM3/3HA:BEM3*) was grown to exponential phase in YM-P medium at 23°C and examined by immunofluorescence using anti-HA antibody. (B and C) Strain M-17 (*cdc12-6*) carrying plasmid YEp13-GFP-BEM3 was grown to exponential phase in liquid SC-Leu medium at 23°C and observed by fluorescence microscopy (B) or shifted to 37°C for 1 h before observation (C). (D) Localization of Rga2p. Strain YEF2291 (*RGA2:GFP/RGA2:GFP*) was grown overnight on a YPD plate at 23°C and observed by fluorescence microscopy. (E–G) Localization of Rga1p and its dependence on septin function. (E) Strain YEF1026 (*bem3*Δ *rga1*Δ) carrying plasmid pRS315-GFP-RGA1 was grown overnight on an SC-Leu plate at 23°C and observed by fluorescence microscopy. (F) Strain YEF1424 (*3HA:RGA1/3HA:RGA1*) was grown to exponential phase in YM-P medium at 23°C and triple stained using anti-HA antibody (top), anti-Cdc11p antibodies (middle), and bisBenzimide (bottom). (G) Strain YEF1418 (*cdc12-6 3HA:RGA1*) was grown to exponential phase in liquid SC-Ura medium at 23°C, shifted to 37°C for 1 h, and triple stained as in F.

Ford and Pringle, 1991; Cid *et al.*, 2001; C. Caruso and J. Pringle, unpublished results). These observations suggest that the transition from a low- to a high-stability state as seen by FRAP may correspond to the development of the higher-order structure that results in the apparent filaments seen in the EM.

Because the initial recruitment step appears to depend on both Cdc42p and Cdc24p (Pringle *et al.*, 1995; Cid *et al.*, 2001; Gladfelter *et al.*, 2002; H.B. Kim, B.K. Haarer, and J.R. Pringle, unpublished results), it presumably depends on the presence of Cdc42p-GTP (Figure 10A). However, to our knowledge, at present there is no strong evidence for the involvement of the Cdc42p GAPs, of a Cdc42p GTPase cycle, or of any other known effector in this step. It is also not yet clear whether the septins are recruited directly into a ring at the presumptive bud site or first form patches and/or a cap that is rapidly converted into a ring before bud emergence (Figure 10A). In the former case, the septin patches and caps observed in the elongated buds of various mutants (Figure 10B) would be strictly abnormal structures that develop in the absence of important assembly factors, whereas in the latter case, these structures would represent the abnormal persistence of normal intermediates in the assembly of the mature septin ring. In either case, however, the continued lability of these structures as seen by FRAP would be expected. It should also be noted that because the assembly step may have two substeps (patches/cap to ring; ring to more stable ring/hourglass structure), it remains unclear whether all of the assembly factors cited above really function at precisely the same stage in the assembly process.

Mode of Cdc42p-GAP Action in Promoting Septin Assembly

An important question is whether the Cdc42p GAPs promote septin assembly solely via their GAP activity (i.e., by

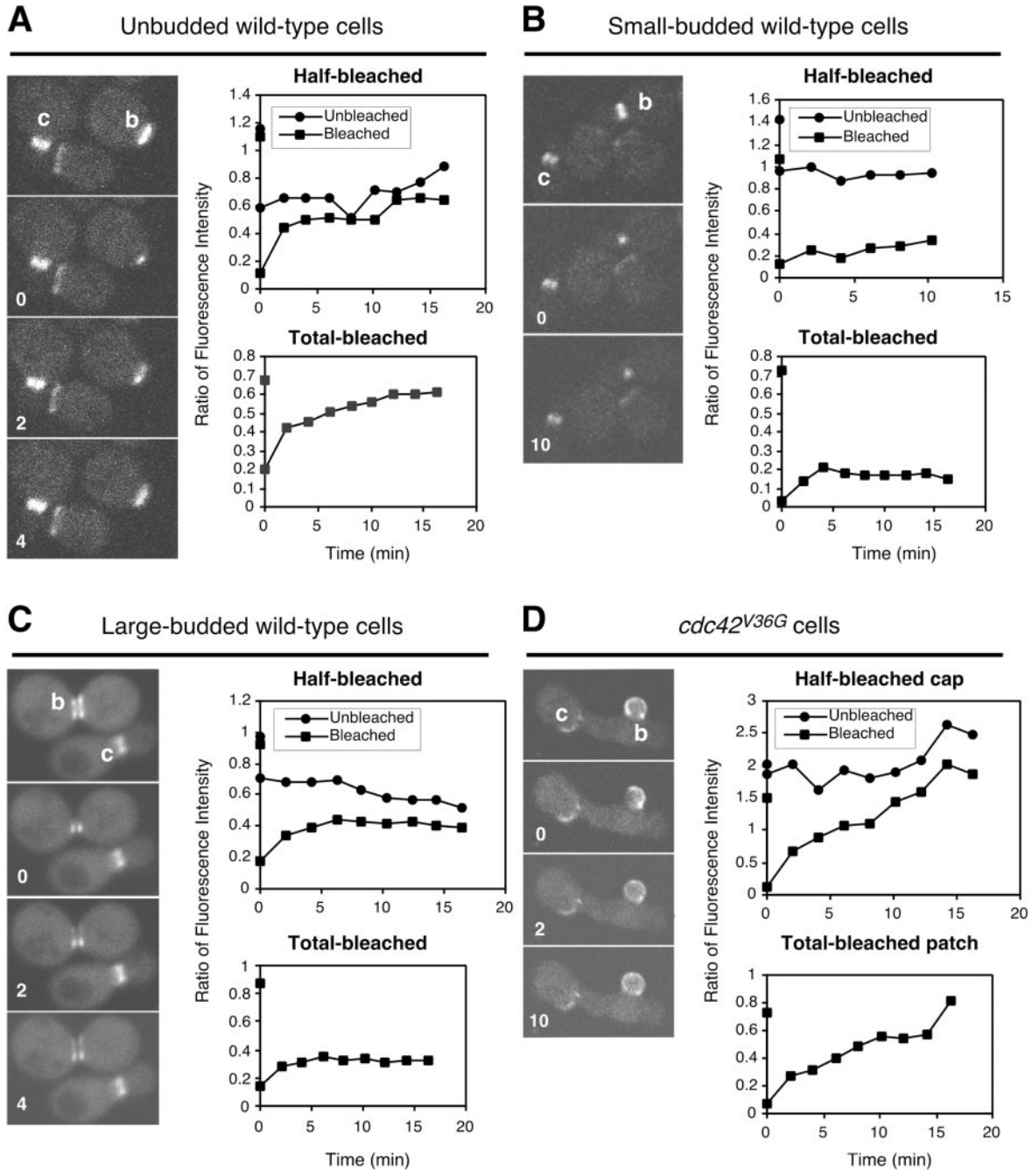

Figure 8. FRAP studies of septin dynamics in wild-type and mutant cells. All strains carried plasmid pRS316-CDC3-GFP. In some experiments, half the septin structure of interest was bleached, and the subsequent changes in fluorescence of both the bleached and unbleached portions of the structure were monitored; in other experiments, the entire septin structure was bleached before monitoring recovery. In each panel, a representative series of images for a half-bleached structure is shown together with the corresponding quantitation; the quantitative data for a representative total-bleached structure are also shown. b, the cells that were bleached; c, the unbleached control cells used to normalize the fluorescence values from the bleached cells (see MATERIALS AND METHODS). Note that in one case (D, half-bleached), the unbleached septin structure used as control was actually on the same cell as the bleached structure. (A–C) Wild-type strain YEF473A. (A) Unbudded cells. Similar data (i.e., extensive recovery of fluorescence within 2 min) were obtained with seven half-bleached and 12 total-bleached cells. (B) Small-budded cells. Similar data (i.e., very little recovery of fluorescence even after 10 min) were obtained with 10 half-bleached and 7 total-bleached cells. Cells with medium-sized buds behaved similarly (unpublished data). (C) Large-budded cells; all cells examined had septa visible by DIC and thus had already completed cytokinesis but not cell separation. Similar data were obtained with 6 half-bleached (all showed extensive recovery of fluorescence by 4 min) and 15 total-bleached (all showed only limited recovery of fluorescence even after 10 min) cells. (D) *cdc42*^{V36G} mutant strain YEF2921 and *bem3*Δ *rga1*Δ *rga2*Δ triple-mutant strain YEF2380. Abnormal septin caps and patches were examined; similar data (i.e., extensive recovery of fluorescence within 4 min and further recovery by 10 min) were obtained with five caps (all half-bleached) and five patches (all total-bleached). One half-bleached cap and two total-bleached patches recovered fluorescence more slowly. Structures in the two strains behaved similarly; the data shown were obtained with strain YEF2921.

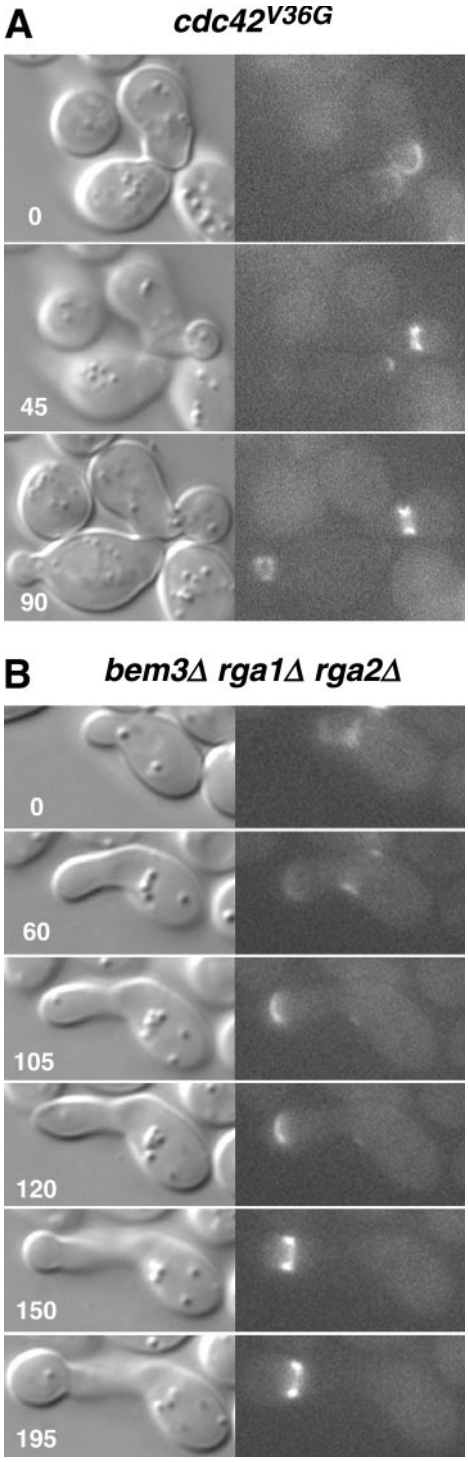

Figure 9. Correlation between the pattern of septin organization and the pattern of bud growth. Time-lapse microscopy was performed at 23°C on *cdc42*^{V36G} strain YEF2921 (A) and *bem3*Δ *rga1*Δ *rga2*Δ strain YEF2380 (B) carrying plasmid pRS316-CDC3-GFP. Times are indicated in minutes.

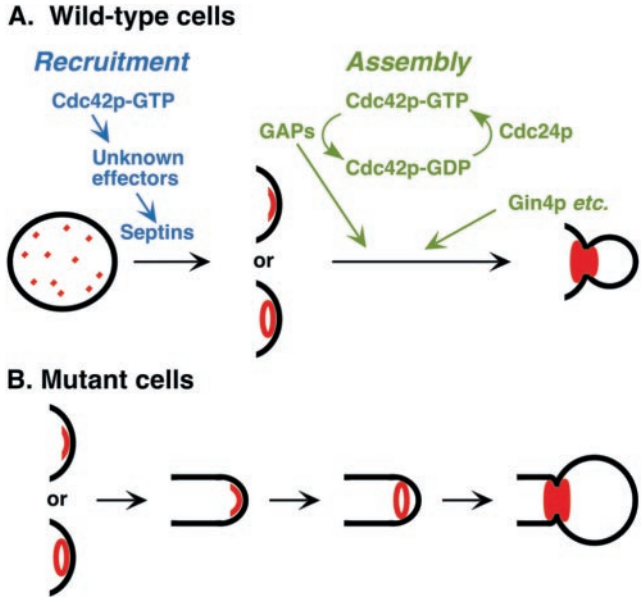

Figure 10. Two-step model for formation of the mature septin ring. Septin monomers or oligomers are recruited to the presumptive bud site in a process that appears to depend on Cdc42p-GTP but for which the effectors are unknown. It is also not known whether the septins are recruited directly into a ring or first form patches and/or a cap that then converts to a ring before bud emergence. (A) In wild-type cells, the labile (capable of rapid subunit exchange) structure(s) present before bud emergence assembles efficiently into a more stable structure at about the time of bud emergence; this assembly may coincide with the conversion of the initial septin ring into the hourglass-shaped structure of the budded cell. The assembly process also appears to depend on Cdc42p and on multiple factors (the Cdc42p GAPs, Gin4p, Cla4p, Bni5p, Elm1p, Nap1p) that are at least partially redundant in function based on the synthetic phenotypes of double mutants. It is not clear whether all of these factors function at precisely the same stage in the assembly process (see text). (B) In various mutants, the assembly of the stable structure is prevented or delayed, and a labile cap or patches can form and/or persist for an extended period. The eventual formation of a more normal, stable ring is accompanied by a shift to a more normal pattern of bud growth. See text for additional details.

accelerating the GTPase cycle of Cdc42p) or whether they also (or instead) have some type of effector function. Gladfelter *et al.* (2002) have argued for a model of the former type, proposing that the Cdc42p GTPase cycle might function in adding septin subunits to a growing assembly much as the EF-Tu/EF-1α GTPase cycle functions in adding amino acids to a growing polypeptide chain. In this context, they interpreted the inability of Rga1p^{K872A} to suppress the septin-specific *cdc42* alleles as reflecting its loss of GAP activity. However, this argument is weakened by the observation that Rga1p^{K872A} also displays a greatly reduced ability to interact with Cdc42p and does not discriminate between Cdc42p-GTP and Cdc42p-GDP (Gladfelter *et al.*, 2002), so that its lack of suppressor function (Figure 2; Gladfelter *et al.*, 2002) might simply reflect its inability to interact normally with Cdc42p.

In support of their model, Gladfelter *et al.* (2002) also stressed the observation that Bem3p and Rga1p/Rga2p appear to be at least partially redundant for their role in septin assembly despite having little or no homology outside of their GAP domains. Despite the apparent strength of this argument, we nonetheless prefer a model in which the GAPs function at least in part as effectors, for several reasons. First, the effectiveness of GAP overexpression in restoring the formation of septin rings of seemingly normal structure in septin mutants (Figures 1C and 2B) seems difficult to explain

solely by an increased rate of subunit addition (produced by an accelerated GTPase cycle). Second, the three GAPs differ greatly in their abilities to suppress both septin mutations and septin-specific *cdc42* mutations (Figure 1; Gladfelter *et al.*, 2002), although in vitro assays showed no significant differences in their efficacies as GAPs (Smith *et al.*, 2002). Finally, Gladfelter *et al.* (2002) observed that overexpression of Rga1p could effectively suppress both $cdc42^{V36T}$ and $cdc42^{Y32H}$, although in GAP assays, Rga1p could stimulate the GTPase activity of $Cdc42p^{V36T}$ but not of $Cdc42p^{Y32H}$. However, it should be noted that the latter two arguments are both subject to the caveat that the GAP assays are performed with isolated GAP domains in vitro and may not accurately reflect the activities of the full-length proteins at physiological concentrations in vivo.

It should also be noted that the GAPs-as-GAPs and GAPs-as-effectors models are not mutually exclusive. In particular, the GAPs could contribute to septin-ring formation both by driving the Cdc42p GTPase cycle and thus promoting subunit addition (as proposed by Gladfelter *et al.*, 2002) and by serving an additional effector role in the proper assembly of the added subunits (Figure 10A). It also remains possible that the Cdc42p GTPase cycle (driven by the GAPs) is involved in the initial recruitment of septin subunits to the appropriate site in the cell cortex. Further studies will be required to discriminate among these possibilities and to define the nature of the putative effector role of the GAPs.

Role of the Septins in Bud Morphogenesis

It has long been known that septin mutants produce hyperpolarized, abnormally elongated buds (Hartwell, 1971; Adams and Pringle, 1984). Recent observations have suggested that at least part of the reason for this is that septin mutants have a transient, Swe1p-dependent delay in the G2-M transition, which results in a delay in the switch from polarized to isotropic growth of the bud (Carroll *et al.*, 1998; Barral *et al.*, 1999; Shulewitz *et al.*, 1999; Longtine *et al.*, 2000). However, microscopic (including time-lapse) observations have also suggested that the buds formed by septin mutants are already abnormal in shape when they first emerge, before a G2-M delay could be playing a role (Adams and Pringle, 1984; J.R. Pringle, unpublished results), and thus that the septins must play a more direct role in determining the pattern of bud growth. Our time-lapse observations on the $cdc42^{V36G}$ and *bem3 rga1 rga2* mutants appear to support this hypothesis. Individual mutant cells showed widely different delays in the conversion of the septin caps into normal-looking septin rings. Irrespective of the time of cap-to-ring conversion in a given cell, this conversion was immediately followed by a striking change in the pattern of bud growth, from continued tip elongation to more nearly isotropic growth leading to the formation of a bud of approximately normal shape (Figures 9 and 10B). The observation that deleting *SWE1* had little effect on the elongated-bud phenotypes of the *bem3 rga1 rga2* and *bem3 rga1 gin4* mutants (see RESULTS) further supports the hypothesis that the septins play a direct role in determining the normal pattern of bud growth. The nature of this role remains to be established and might involve interactions with the actin cytoskeleton, with the secretory system, or both.

ACKNOWLEDGMENTS

We thank Amy Gladfelter, Danny Lew, Greg Smith, George Sprague, and Sally Zigmond for stimulating discussions, communication of results before publication, and/or helpful comments on the manuscript. We also thank Alan Bender, Danny Lew, and George Sprague for plasmids, and Chris Dravis, Nathan Shaner, Jeff Robens, and Carlo Caruso for excellent technical assistance. This work was supported by National Institutes of Health Grants GM 59216 (E.B.) and GM31006 (J.R.P.).

REFERENCES

Adams, A.E.M., and Pringle, J.R. (1984). Relationship of actin and tubulin distribution to bud growth in wild-type and morphogenetic-mutant *Saccharomyces cerevisiae.* J. Cell Biol. *98,* 934–945.

Ayscough, K.R., Stryker, J., Pokala, N., Sanders, M., Crews, P., and Drubin, D.G. (1997). High rates of actin filament turnover in budding yeast and roles for actin in establishment and maintenance of cell polarity revealed using the actin inhibitor Latrunculin-A. J. Cell Biol. *137,* 399–416.

Barral, Y., Parra, M., Bidlingmaier, S., and Snyder, M. (1999). Nim1-related kinases coordinate cell cycle progression with the organization of the peripheral cytoskeleton in yeast. Genes Dev. *13,* 176–187.

Barral, Y., Mermall, V., Mooseker, M.S., and Snyder, M. (2000). Compartmentalization of the cell cortex by septins is required for maintenance of cell polarity in yeast. Mol. Cell *5,* 841–851.

Baudin, A., Ozier-Kalogeropoulos, O., Denouel, A., Lacroute, F., and Cullin, C. (1993). A simple and efficient method for direct gene deletion in *Saccharomyces cerevisiae.* Nucleic Acids Res. *21,* 3329–3330.

Beites, C.L., Xie, H., Bowser, R., and Trimble, W.S. (1999). The septin CDCrel-1 binds syntaxin and inhibits exocytosis. Nat. Neurosci. *2,* 434–439.

Bi, E., and Pringle, J.R. (1996). ZDS1 and *ZDS2*, genes whose products may regulate Cdc42p in *Saccharomyces cerevisiae.* Mol. Cell. Biol. *16,* 5264–5275.

Bi, E., Maddox, P., Lew, D.J., Salmon, E.D., McMillan, J.N., Yeh, E., and Pringle, J.R. (1998). Involvement of an actomyosin contractile ring in *Saccharomyces cerevisiae* cytokinesis. J. Cell Biol. *142,* 1301–1312.

Bi, E., Chiavetta, J.B., Chen, H., Chen, G.-C., Chan, C.S.M., and Pringle, J.R. (2000). Identification of novel, evolutionarily conserved Cdc42p-interacting proteins and of redundant pathways linking Cdc24p and Cdc42p to actin polarization in yeast. Mol. Biol. Cell *11,* 773–793.

Bouquin, N., Barral, Y., Courbeyrette, R., Blondel, M., Snyder, M., and Mann, C. (2000). Regulation of cytokinesis by the Elm1 protein kinase in *Saccharomyces cerevisiae.* J. Cell Sci. *113,* 1435–1445.

Byers, B. (1981). Cytology of the yeast life cycle. In: The Molecular Biology of the Yeast *Saccharomyces*: Life Cycle and Inheritance, ed. J.N. Strathern, E.W. Jones, and J.R. Broach, Cold Spring Harbor, NY: Cold Spring Harbor Laboratory Press, 59–96.

Byers, B., and Goetsch, L. (1976a). A highly ordered ring of membrane-associated filaments in budding yeast. J. Cell Biol. *69,* 717–721.

Byers, B., and Goetsch, L. (1976b). Loss of the filamentous ring in cytokinesis-defective mutants of budding yeast. J. Cell Biol. *70,* 35a.

Carroll, C.W., Altman, R., Schieltz, D., Yates, J. R., III, and Kellogg, D. (1998). The septins are required for the mitosis-specific activation of the Gin4 kinase. J. Cell Biol. *143,* 709–717.

Caviston, J.P., Tcheperegine, S.E., and Bi, E. (2002). Singularity in budding: a role for the evolutionarily conserved small GTPase Cdc42p. Proc. Natl. Acad. Sci. USA *99,* 12185–12190.

Chant, J., Mischke, M., Mitchell, E., Herskowitz, I., and Pringle, J.R. (1995). Role of Bud3p in producing the axial budding pattern of yeast. J. Cell Biol. *129,* 767–778.

Christianson, T.W., Sikorski, R.S., Dante, M., Shero, J.H., and Hieter, P. (1992). Multifunctional yeast high-copy-number shuttle vectors. Gene *110,* 119–122.

Cid, V.J., Adamiková, L., Sánchez, M., Molina, M., and Nombela, C. (2001). Cell cycle control of septin ring dynamics in the budding yeast. Microbiology *147,* 1437–1450.

Cvrcková, F., De Virgilio, C., Manser, E., Pringle, J.R., and Nasmyth, K. (1995). Ste20-like protein kinases are required for normal localization of cell growth and for cytokinesis in budding yeast. Genes Dev. *9,* 1817–1830.

DeMarini, D.J., Adams, A.E.M., Fares, H., De Virgilio, C., Valle, G., Chuang, J.S., and Pringle, J.R. (1997). A septin-based hierarchy of proteins required for localized deposition of chitin in the *Saccharomyces cerevisiae* cell wall. J. Cell Biol. *139,* 75–93.

Dent, J., Kato, K., Peng, X.-R., Martinez, C., Cattaneo, M., Poujol, C., Nurden, P., Nurden, A., Trimble, W.S., and Ware, J. (2002). A prototypic platelet septin and its participation in secretion. Proc. Natl. Acad. Sci. USA *99,* 3064–3069.

De Virgilio, C., DeMarini, D.J., and Pringle, J.R. (1996). SPR28, a sixth member of the septin gene family in *Saccharomyces cerevisiae* that is expressed specifically in sporulating cells. Microbiology *142,* 2897–2905.

Dobbelaere, J., Gentry, M.S., Hallberg, R.L., and Barral, Y. (2003). Phosphorylation-dependent regulation of septin dynamics during the cell cycle. Dev. Cell *4,* 345–357.

Fares, H., Goetsch, L., and Pringle, J.R. (1996). Identification of a developmentally regulated septin and involvement of the septins in spore formation in *Saccharomyces cerevisiae.* J. Cell Biol. *132,* 399–411.

Field, C.M., and Kellogg, D. (1999). Septins: cytoskeletal polymers or signalling GTPases? Trends Cell Biol. *9,* 387–394.

Field, C.M., Al-Awar, O., Rosenblatt, J., Wong, M.L., Alberts, B., and Mitchison, T.J. (1996). A purified *Drosophila* septin complex forms filaments and exhibits GTPase activity. J. Cell Biol. *133,* 605–616.

Ford, S.K., and Pringle, J.R. (1991). Cellular morphogenesis in the *Saccharomyces cerevisiae* cell cycle: localization of the *CDC11* gene product and the timing of events at the budding site. Dev. Genet. *12,* 281–292.

Frazier, J.A., Wong, M.L., Longtine, M.S., Pringle, J.R., Mann, M., Mitchison, T.J., and Field, C. (1998). Polymerization of purified yeast septins: evidence that organized filament arrays may not be required for septin function. J. Cell Biol. *143,* 737–749.

Gietz, R.D., and Sugino, A. (1988). New yeast-*Escherichia coli* shuttle vectors constructed with in vitro mutagenized yeast genes lacking six-base pair restriction sites. Gene *74,* 527–534.

Gladfelter, A.S., Moskow, J.J., Zyla, T.R., and Lew, D.J. (2001a). Isolation and characterization of effector-loop mutants of *CDC42* in yeast. Mol. Biol. Cell *12,* 1239–1255.

Gladfelter, A.S., Pringle, J.R., and Lew, D.J. (2001b). The septin cortex at the yeast mother-bud neck. Curr. Opin. Microbiol. *4,* 681–689.

Gladfelter, A.S., Bose, I., Zyla, T.R., Bardes, E.S.G., and Lew, D.J. (2002). Septin ring assembly involves cycles of GTP loading and hydrolysis by Cdc42p. J. Cell Biol. *156,* 315–326.

Guthrie, C., and Fink, G.R. (eds.) (1991). Guide to yeast genetics and molecular biology. In: Methods in Enzymology, vol 194. San Diego: Academic Press.

Haarer, B.K., and Pringle, J.R. (1987). Immunofluorescence localization of the *Saccharomyces cerevisiae CDC12* gene product to the vicinity of the 10-nm filaments in the mother-bud neck. Mol. Cell. Biol. *7,* 3678–3687.

Harkins, H.A., Pagé, N., Schenkman, L.R., De Virgilio, C., Shaw, S., Bussey, H., and Pringle, J.R. (2001). Bud8p and Bud9p, proteins that may mark the sites for bipolar budding in yeast. Mol. Biol. Cell *12,* 2497–2518.

Hartwell, L.H. (1971). Genetic control of the cell division cycle in yeast. IV. Genes controlling bud emergence and cytokinesis. Exp. Cell Res. *69,* 265–276.

Hsu, S.-C., Hazuka, C.D., Roth, R., Foletti, D.L., Heuser, J., and Scheller, R.H. (1998). Subunit composition, protein interactions, and structures of the mammalian brain sec6/8 complex and septin filaments. Neuron *20,* 1111–1122.

Johnson, D.I. (1999). Cdc *42,* an essential Rho-type GTPase controlling eukaryotic cell polarity. Microbiol. Mol. Biol. Rev. *63,* 54–105.

Kartmann, B., and Roth, D. (2001). Novel roles for mammalian septins: from vesicle trafficking to oncogenesis. J. Cell Sci. *114,* 839–844.

Kim, H.B., Haarer, B.K., and Pringle, J.R. (1991). Cellular morphogenesis in the *Saccharomyces cerevisiae* cell cycle: localization of the *CDC3* gene product and the timing of events at the budding site. J. Cell Biol. *112,* 535–544.

Kinoshita, M., Kumar, S., Mizoguchi, A., Ide, C., Kinoshita, A., Haraguchi, T., Hiraoka, Y., and Noda, M. (1997). Nedd5, a mammalian septin, is a novel cytoskeletal component interacting with actin-based structures. Genes Dev. *11,* 1535–1547.

Kinoshita, M., Field, C.M., Coughlin, M.L., Straight, A.F., and Mitchison, T.J. (2002). Self- and actin-templated assembly of mammalian septins. Dev. Cell *3,* 791–802.

Kozminski, K.G., Chen, A.J., Rodal, A.A., and Drubin, D.G. (2000). Functions and functional domains of the GTPase Cdc42p. Mol. Biol. Cell *11,* 339–354.

Lee, P.R., Song, S., Ro, H.-S., Park, C.J., Lippincott, J., Li, R., Pringle, J.R., De Virgilio, C., Longtine, M.S., and Lee, K.S. (2002). Bni5p, a septin-interacting protein, is required for normal septin function and cytokinesis in *Saccharomyces cerevisiae.* Mol. Cell. Biol. *22,* 6906–6920.

Lew, D.J., and Reed, S.I. (1995). A cell cycle checkpoint monitors cell morphogenesis in budding yeast. J. Cell Biol. *129,* 739–749.

Li, R., Zhang, B., and Zheng, Y. (1997). Structural determinants required for the interaction between Rho GTPase and the GTPase-activating domain of p190. J. Biol. Chem. *272,* 32830–32835.

Lillie, S.H., and Pringle, J.R. (1980). Reserve carbohydrate metabolism in *Saccharomyces cerevisiae*: responses to nutrient limitation. J. Bacteriol. *143,* 1384–1394.

Lippincott, J., and Li, R. (1998). Sequential assembly of myosin II, an IQGAP-like protein, and filamentous actin to a ring structure involved in budding yeast cytokinesis. J. Cell Biol. *140,* 355–366.

Lippincott, J., Shannon, K.B., Shou, W., Deshaies, R.J., and Li, R. (2001). The Tem1 small GTPase controls actomyosin and septin dynamics during cytokinesis. J. Cell Sci. *114,* 1379–1386.

Longtine, M.S., DeMarini, D.J., Valencik, M.L., Al-Awar, O.S., Fares, H., De Virgilio, C., and Pringle, J.R. (1996). The septins: roles in cytokinesis and other processes. Curr. Opin. Cell Biol. *8,* 106–119.

Longtine, M.S., Fares, H., and Pringle, J.R. (1998a). Role of the yeast Gin4p protein kinase in septin assembly and the relationship between septin assembly and septin function. J. Cell Biol. *143,* 719–736.

Longtine, M.S., McKenzie III, A., DeMarini, D.J., Shah, N.G., Wach, A., Brachat, A., Philippsen, P., and Pringle, J.R. (1998b). Additional modules for versatile and economical PCR-based gene deletion and modification in *Saccharomyces cerevisiae.* Yeast *14,* 953–961.

Longtine, M.S., Theesfeld, C.L., McMillan, J.N., Weaver, E., Pringle, J.R., and Lew, D.J. (2000). Septin-dependent assembly of a cell cycle-regulatory module in *Saccharomyces cerevisiae.* Mol. Cell. Biol. *20,* 4049–4061.

Macara, I.G., *et al.* (2002). Mammalian septins nomenclature. Mol. Biol. Cell *13,* 4111–4113.

Mendoza, M., Hyman, A.A., and Glotzer, M. (2002). GTP binding induces filament assembly of a recombinant septin. Curr. Biol. *12,* 1858–1863.

Mino, A., Tanaka, K., Kamei, T., Umikawa, M., Fujiwara, T., and Takai, Y. (1998). Shs1p: a novel member of septin that interacts with Spa2p, involved in polarized growth in *Saccharomyces cerevisiae.* Biochem. Biophys. Res. Comm. *251,* 732–736.

Momany, M., Zhao, J., Lindsey, R., and Westfall, P.J. (2001). Characterization of the *Aspergillus nidulans* septin (*asp*) gene family. Genetics *157,* 969–977.

Neufeld, T.P., and Rubin, G.M. (1994). The Drosophila *peanut* gene is required for cytokinesis and encodes a protein similar to yeast putative bud neck filament proteins. Cell *77,* 371–379.

Nguyen, T.Q., Sawa, H., Okano, H., and White, J.G. (2000). The *C. elegans* septin genes, unc-59 and unc-61, are required for normal postembryonic cytokineses and morphogenesis but have no essential function in embryogenesis. J. Cell Sci. *113,* 3825–3837.

Pringle, J.R., Adams, A.E.M., Drubin, D.G., and Haarer, B.K. (1991). Immunofluorescence methods for yeast. Methods Enzymol. *194,* 565–602.

Pringle, J.R., Bi, E., Harkins, H.A., Zahner, J.E., De Virgilio, C., Chant, J., Corrado, K., and Fares, H. (1995). Establishment of cell polarity in yeast. Cold Spring Harbor Symp. Quant. Biol. *60,* 729–744.

Pruyne, D., and Bretscher, A. (2000). Polarization of cell growth in yeast. I. Establishment and maintenance of polarity states. J. Cell Sci. *113,* 365–375.

Richman, T.J., Sawyer, M.M., and Johnson, D.I. (1999). The Cdc42p GTPase is involved in a G2/M morphogenetic checkpoint regulating the apical-isotropic switch and nuclear division in yeast. J. Biol. Chem. *274,* 16861–16870.

Richman, T.J., Sawyer, M.M., and Johnson, D.I. (2002). Saccharomyces cerevisiae Cdc42p localizes to cellular membranes and clusters at sites of polarized growth. Eukaryotic Cell *1,* 458–468.

Rose, A.B., and Broach, J.R. (1990). Propagation and expression of cloned genes in yeast: 2-μm circle based vectors. Methods Enzymol. *185,* 234–279.

Rothstein, R. (1991). Targeting, disruption, replacement, and allele rescue: integrative DNA transformation in yeast. Methods Enzymol. *194,* 281–301.

Sambrook, J., Fritsch, E.F., and Maniatis, T. (1989). Molecular Cloning: A Laboratory Manual. Cold Spring Harbor, NY: Cold Spring Harbor Laboratory Press.

Sanders, S.L., and Herskowitz, I. (1996). The Bud4 protein of yeast, required for axial budding, is localized to the mother/bud neck in a cell cycle-dependent manner. J. Cell Biol. *134,* 413–427.

Schenkman, L.R., Caruso, C., Pagé, N., and Pringle, J.R. (2002). The role of cell cycle-regulated expression in the localization of spatial landmark proteins in yeast. J. Cell Biol. *156,* 829–841.

Shulewitz, M.J., Inouye, C.J., and Thorner, J. (1999). Hsl7 localizes to a septin ring and serves as an adaptor in a regulatory pathway that relieves tyrosine phosphorylation of Cdc28 protein kinase in *Saccharomyces cerevisiae.* Mol. Cell. Biol. *19,* 7123–7137.

Sikorski, R.S., and Hieter, P. (1989). A system of shuttle vectors and yeast host strains designed for efficient manipulation of DNA in *Saccharomyces cerevisiae.* Genetics *122,* 19–27.

Smith, G.R., Givan, S.A., Cullen, P., and Sprague, G.F., Jr. (2002). GTPase-activating proteins for Cdc42. Eukaryotic Cell *1,* 469–480.

Sreenivasan, A., and Kellogg, D. (1999). The Elm1 kinase functions in a mitotic signaling network in budding yeast. Mol. Cell. Biol. *19,* 7983–7994.

Stevenson, B.J., Ferguson, B., De Virgilio, C., Bi, E., Pringle, J.R., Ammerer, G., and Sprague, G.F., Jr. (1995). Mutation of *RGA1*, which encodes a putative GTPase-activating protein for the polarity-establishment protein Cdc42p, activates the pheromone-response pathway in the yeast *Saccharomyces cerevisiae.* Genes Dev. *9,* 2949–2963.

Takizawa, P.A., DeRisi, J.L., Wilhelm, J.E., and Vale, R.D. (2000). Plasma membrane compartmentalization in yeast by messenger RNA transport and a septin diffusion barrier. Science *290,* 341–344.

Trimble, W.S. (1999). Septins: a highly conserved family of membrane-associated GTPases with functions in cell division and beyond. J. Membr. Biol. *169,* 75–81.

Tyers, M., Tokiwa, G., and Futcher, B. (1993). Comparison of the *Saccharomyces cerevisiae* G_1 cyclins: Cln3 may be an upstream activator of Cln1, Cln2 and other cyclins. EMBO J. *12,* 1955–1968.

Vallen, E.A., Caviston, J., and Bi, E. (2000). Roles of Hof1p, Bni1p, Bnr1p, and Myo1p in cytokinesis in *Saccharomyces cerevisiae.* Mol. Biol. Cell *11,* 593–611.

Weiss, E.L., Bishop, A.C., Shokat, K.M., and Drubin, D.G. (2000). Chemical genetic analysis of the budding-yeast p21-activated kinase Cla4p. Nat. Cell Biol. *2,* 677–685.

Westfall, P.J., and Momany, M. (2002). Aspergillus nidulans septin AspB plays pre- and postmitotic roles in septum, branch, and conidiophore development. Mol. Biol. Cell *13,* 110–118.

Yeh, E., Skibbens, R.V., Cheng, J.W., Salmon, E.D., and Bloom, K. (1995). Spindle dynamics and cell cycle regulation of dynein in the budding yeast, *Saccharomyces cerevisiae.* J. Cell Biol. *130,* 687–700.

Zheng, Y., Hart, M.J., Shinjo, K., Evans, T., Bender, A., and Cerione, R.A. (1993). Biochemical comparisons of the *Saccharomyces cerevisiae* Bem2 and Bem3 proteins. Delineation of a limit Cdc42 GTPase-activating protein domain. J. Biol. Chem. *268,* 24629–24634.

Ziman, M., Preuss, D., Mulholland, J., O'Brien, J.M., Botstein, D., and Johnson, D.I. (1993). Subcellular localization of Cdc42p, a *Saccharomyces cerevisiae* GTP-binding protein involved in the control of cell polarity. Mol. Biol. Cell *4,* 1307–1316.